

# **Estimating the Mean Annual Surface Air Temperature at Armagh Observatory, Northern Ireland, and the Global Land-Ocean Temperature Index for Sunspot Cycle 24, the Current Ongoing Sunspot Cycle**

*Robert M. Wilson  
Marshall Space Flight Center, Huntsville, Alabama*

## The NASA STI Program...in Profile

Since its founding, NASA has been dedicated to the advancement of aeronautics and space science. The NASA Scientific and Technical Information (STI) Program Office plays a key part in helping NASA maintain this important role.

The NASA STI Program Office is operated by Langley Research Center, the lead center for NASA's scientific and technical information. The NASA STI Program Office provides access to the NASA STI Database, the largest collection of aeronautical and space science STI in the world. The Program Office is also NASA's institutional mechanism for disseminating the results of its research and development activities. These results are published by NASA in the NASA STI Report Series, which includes the following report types:

- **TECHNICAL PUBLICATION.** Reports of completed research or a major significant phase of research that present the results of NASA programs and include extensive data or theoretical analysis. Includes compilations of significant scientific and technical data and information deemed to be of continuing reference value. NASA's counterpart of peer-reviewed formal professional papers but has less stringent limitations on manuscript length and extent of graphic presentations.
- **TECHNICAL MEMORANDUM.** Scientific and technical findings that are preliminary or of specialized interest, e.g., quick release reports, working papers, and bibliographies that contain minimal annotation. Does not contain extensive analysis.
- **CONTRACTOR REPORT.** Scientific and technical findings by NASA-sponsored contractors and grantees.
- **CONFERENCE PUBLICATION.** Collected papers from scientific and technical conferences, symposia, seminars, or other meetings sponsored or cosponsored by NASA.
- **SPECIAL PUBLICATION.** Scientific, technical, or historical information from NASA programs, projects, and mission, often concerned with subjects having substantial public interest.
- **TECHNICAL TRANSLATION.** English-language translations of foreign scientific and technical material pertinent to NASA's mission.

Specialized services that complement the STI Program Office's diverse offerings include creating custom thesauri, building customized databases, organizing and publishing research results...even providing videos.

For more information about the NASA STI Program Office, see the following:

- Access the NASA STI program home page at <http://www.sti.nasa.gov>
- E-mail your question via the Internet to [help@sti.nasa.gov](mailto:help@sti.nasa.gov)
- Fax your question to the NASA STI Help Desk at 443-757-5803
- Phone the NASA STI Help Desk at 443-757-5802
- Write to:  
NASA STI Help Desk  
NASA Center for AeroSpace Information  
7115 Standard Drive  
Hanover, MD 21076-1320

NASA/TP—2013–217484



# **Estimating the Mean Annual Surface Air Temperature at Armagh Observatory, Northern Ireland, and the Global Land-Ocean Temperature Index for Sunspot Cycle 24, the Current Ongoing Sunspot Cycle**

*Robert M. Wilson  
Marshall Space Flight Center, Huntsville, Alabama*

National Aeronautics and  
Space Administration

Marshall Space Flight Center • Huntsville, Alabama 35812

---

**July 2013**

Available from:

NASA Center for AeroSpace Information  
7115 Standard Drive  
Hanover, MD 21076-1320  
443-757-5802

This report is also available in electronic form at  
<<https://www2.sti.nasa.gov/login/wt/>>



## TABLE OF CONTENTS

1. INTRODUCTION .....	1
2. RESULTS .....	2
2.1 Annual and 10-Year Moving Averages of ASAT, GLOTI, and SSN .....	2
2.2 ASC, PER, Rmax, <SSN>, <ASAT>, and <GLOTI> for SC10–SC23 .....	11
2.3 Behavioral Aspects of ASAT and GLOTI During Rmin and Rmax Years .....	20
2.4 Behavioral Aspects of ASAT AND GLOTI Relative to the AMO Index and the Trend in the Atmospheric Concentration of Carbon Dioxide at Mauna Loa, Hawaii .....	26
3. DISCUSSION AND CONCLUSIONS .....	30
REFERENCES .....	35



## LIST OF FIGURES

1.	Annual (thin jagged line) and 10-yma (thick smoothed line) of (a) ASAT for the interval 1844–2011, (b) GLOTI for the interval 1880–2011, and (c) SSN for the interval 1840–2011 .....	3
2.	Residuals for (a) ASAT and (b) GLOTI, where the residual is simply the difference between the observed annual values and the corresponding 10-yma values (for the same year) .....	5
3.	Distributions of the residuals for (a) ASAT and (b) GLOTI .....	6
4.	Scatter plots of (a) annual values of GLOTI versus ASAT for the interval 1880–2011 and (b) GLOTI versus ASAT using 10-yma values for the interval 1885–2006 .....	7
5.	Variation in <i>fd</i> values of the 10-yma values for (a) ASAT and (b) GLOTI .....	9
6.	Distribution of the <i>fd</i> values for (a) ASAT and (b) GLOTI .....	10
7.	Variation of both the actual cyclic value (the thin dotted line) and the two-cycle moving average (the thick smoothed line) for SC10–SC23 of (a) ASC, (b) PER, (c) Rmax, (d) <SSN>, (e) <ASAT>, and (f) <GLOTI> .....	12
8.	Scatter plots of the cyclic averages of (a) <ASAT> versus Rmax, (b) <GLOTI> versus Rmax, (c) <ASAT> versus <SSN>, and (d) <GLOTI> versus <SSN>, where the numbered filled circles refer to the SC .....	16
9.	Scatter plots of (a) <GLOTI> versus <ASAT> and (b) <SSN> versus Rmax .....	18
10.	Variation of (a) SSN, (b) ASAT, and (c) GLOTI from January 1996–September 2012 and the variation of (d) <SSN>, (e) <ASAT>, and (f) <GLOTI> for elapsed time in years past the sunspot minimum year for SC23 (the unfilled histograms) and SC24 (the filled histograms) .....	19
11.	Yearly averages of (a) Rmin (filled circles) and Rmax (filled triangles), (b) ASAT for Rmin years (filled circles) and Rmax years (filled triangles), and (c) GLOTI for Rmin years (filled circles) and Rmax years (filled triangles) for SC9–SC24 .....	21

## LIST OF FIGURES (Continued)

12.	Scatter plots of (a) Rmax versus Rmin, (b) ASAT (Rmax year) versus ASAT (Rmin year), and (c) GLOTI (Rmax year) versus GLOTI (Rmin year), with the arrows located along the <i>x</i> -axes marking the values in the Rmin year for SC24 .....	22
13.	Cyclic secular trend over SC9–SC23 of (a) ASAT (Rmin year), (b) GLOTI (Rmin year), (c) ASAT (Rmax year), and (d) GLOTI (Rmax year) .....	24
14.	Scatter plots of (a) ASAT (Rmin year) and (b) GLOTI (Rmin year) versus Rmin .....	25
15.	Scatter plots of (a) ASAT (Rmax year) and (b) GLOTI (Rmax year) versus Rmax .....	26
16.	Annual (thin jagged line) and 10-yma (thick smoothed line) of (a) the AMO index and (b) the MLCO2 values for the interval 1950–2011 .....	28
17.	Scatter plots of (a) ASAT and (b) GLOTI against the AMO index for the interval 1950–2006, based on 10-yma values .....	29
18.	Scatter plots of (a) ASAT and (b) GLOTI versus the MLCO2 values for the interval 1964–2006, based on 10-yma values .....	29
19.	Linear fits of (a) <ASAT> and (b) <GLOTI> versus SC for SC12–SC23 .....	31

## LIST OF ABBREVIATIONS, ACRONYMS, AND SYMBOLS

10-yma	10-year moving average
AMO	Atlantic Multidecadal Oscillation
ASAT	Armagh surface air temperature
<ASAT>	average ASAT over the sunspot cycle from sunspot minimum year to the following sunspot minimum year
ASC	ascent duration
CO <sub>2</sub>	carbon dioxide
EN	El Niño
ENSO	El Niño Southern Oscillation
GLOTI	Global Land-Ocean Temperature Index
<GLOTI>	average GLOTI over the sunspot cycle from sunspot minimum year to the following minimum year
LN	La Niña
MLCO2	Mauna Loa carbon dioxide
ONI	Oceanic Niño Index
PER	period
Rmax	maximum amplitude
Rmin	minimum amplitude
SC	sunspot cycle
SSN	sunspot number

## **LIST OF ABBREVIATIONS, ACRONYMS, AND SYMBOLS (Continued)**

<SSN>	the average SSN over the sunspot cycle from sunspot minimum year to the following sunspot minimum year
TP	Technical Publication
VEI	Volcanic Explosivity Index

## NOMENCLATURE

$cl$	confidence level
$fd$	first difference
$P$	probability
$r$	coefficient of correlation
$r^2$	coefficient of determination
$sd$	standard deviation
$se$	standard error of estimate
$t$	year
$x$	independent variable in regression equation
$y$	dependent variable in regression equation
$y'$	alternate regressions
$z$	normal deviate of the sample





## TECHNICAL PUBLICATION

# ESTIMATING THE MEAN ANNUAL SURFACE AIR TEMPERATURE AT ARMAGH OBSERVATORY, NORTHERN IRELAND, AND THE GLOBAL LAND-OCEAN TEMPERATURE INDEX FOR SUNSPOT CYCLE 24, THE CURRENT ONGOING SUNSPOT CYCLE

## 1. INTRODUCTION

As noted by Gray et al., Sir William Herschel was the first to suggest a possible close connection between the Sun and the Earth's climate.<sup>1-7</sup> The Sun, being the source of energy that impacts and drives the Earth's climate system, displays a variety of changes over both short and long term time scales, the most obvious examples being the somewhat regular waxing and waning of sunspots with time (i.e., the sunspot cycle (SC)), first described by Samuel Heinrich Schwabe,<sup>8</sup> a German apothecary and amateur astronomer who observed the Sun from Dessau, Germany,<sup>9-13</sup> and the now well established variation of the Sun's irradiance over the SC.<sup>14-24</sup>

Other factors related to the SC have been linked to changes in climate as well. Some of these other factors include the role of cosmic rays and the solar wind (i.e., the geomagnetic cycle) on climate,<sup>25-43</sup> as well as the apparent close association between trends in global and northern hemispheric temperature and the length of the SC,<sup>44-52</sup> although some investigators have described the inferred association between climate and, in particular, SC length as now being weak.<sup>53-60</sup>

More recently, Solheim et al. have reported on the relation between SC length and the average temperature in the same and immediately following SC for a number of meteorological stations in Norway and in the North Atlantic region.<sup>61</sup> They noted that while they found no significant trend (correlation) between SC length and the average temperature when measured for the same cycle, in contrast, they found a significant negative trend when SC length was compared with the following cycle's average temperature. From this observation, they suggested that average northern hemispheric temperature during the present ongoing SC (SC24) will be lower by about 0.9 °C than was seen in SC23 (spanning 1996-2007, based on yearly averages of sunspot number (SSN), and onset for SC24 occurring in 2008).

The purpose of this Technical Publication (TP) is to examine the annual variations of the Armagh surface air temperature (ASAT) and the Global Land-Ocean Temperature Index (GLOTI) in relation to SSN and the SC in order to determine their likely values during SC24. Hence, it may provide insight as to whether solar forcing of global temperature is now lessening as a contributor to global warming, thereby indicating a possible cooling in the near term immediate future that potentially could ameliorate the effect of increased anthropogenic warming.<sup>57,58,62-66</sup>

## 2. RESULTS

### 2.1 Annual and 10-Year Moving Averages of ASAT, GLOTI, and SSN

Figure 1 displays the annual (January–December; thin jagged line) and 10-year moving averages (10-yma) (thick smoothed line) of (a) ASAT, (b) GLOTI, and (c) SSN for the interval 1840–2011 (although annual values for these parameters are now known through 2012, it should be noted that at the time of writing, the data were available only through September 2012, which forms the basis for this study). For ASAT, the values are available for the years 1844–2011, while for GLOTI the values are available for the years 1880–2011. For SSN, the values are available for the entire interval 1840–2011; however, they are considered most reliable only for the interval 1882–2011. Prior to 1882, the values of SSN are considered less reliable based on a comparison of Zürich or Wolf SSN (now International SSN) against group SSN.<sup>11,67–73</sup> In each subpanel, the mean, standard deviation (*sd*), and low- and high-annual values are given, as well as their years of occurrence. Individual SCs are identified across the bottom in figure 1(c). Hence, for their individual intervals of data availability, ASAT is found to average about  $9.25 \pm 0.55$  °C (i.e., the mean  $\pm 1$  *sd* interval), GLOTI about  $-0.02 \pm 0.27$  °C, and SSN about  $55 \pm 43.4$ , and the ranges of annual values are found to span 7.4 (in 1879) to 10.6 °C (in 2007) for ASAT,  $-0.42$  (in 1907) to  $0.63$  °C (in 2010) for GLOTI, and 1.4 (in 1913, minimum amplitude (Rmin) for SC15) to 190.2 (in 1957, maximum amplitude (Rmax) for SC19) for SSN. The peak annual values of ASAT and GLOTI are about 2.4 *sd* higher than their respective long term means, while the peak annual mean for SSN is about 3 *sd* higher than its long term mean. The lows are respectively about 3.4, 1.5, and 1.2 *sd* lower than their long term means.

The ASAT is one of the longest, continuous, thermometer-based temperature records available for study.<sup>45,74–79</sup> The Armagh Observatory lies about 1 km northeast of the center of the ancient city of Armagh, Northern Ireland, being located at 54°21'12" N. and 6°38'54" W. It is situated about 64 m above sea level at the top of a small hill in an estate of natural woodland and parkland that measures about 7 ha. Previous studies have shown that its rural environment has ensured that the temperature measurements suffer little or no urban microclimatic effects and that the measured temperature record can serve as a good proxy for monitoring long term trends in both northern hemispheric and global annual mean temperature.<sup>76,80</sup> The data for the ASAT are available online at <<http://climate.arm.ac.uk/scans>>.

The GLOTI is a measure of the anomaly in global land-ocean temperatures relative to the base period of 1951–1980, where the data are taken from the Global Historical Climate Network, version 3, using elimination of outliers and homogeneity adjustment. The data (January–December averages) for the GLOTI are available online at <<http://data.giss.nasa.gov/gistemp>>.<sup>81–83</sup>

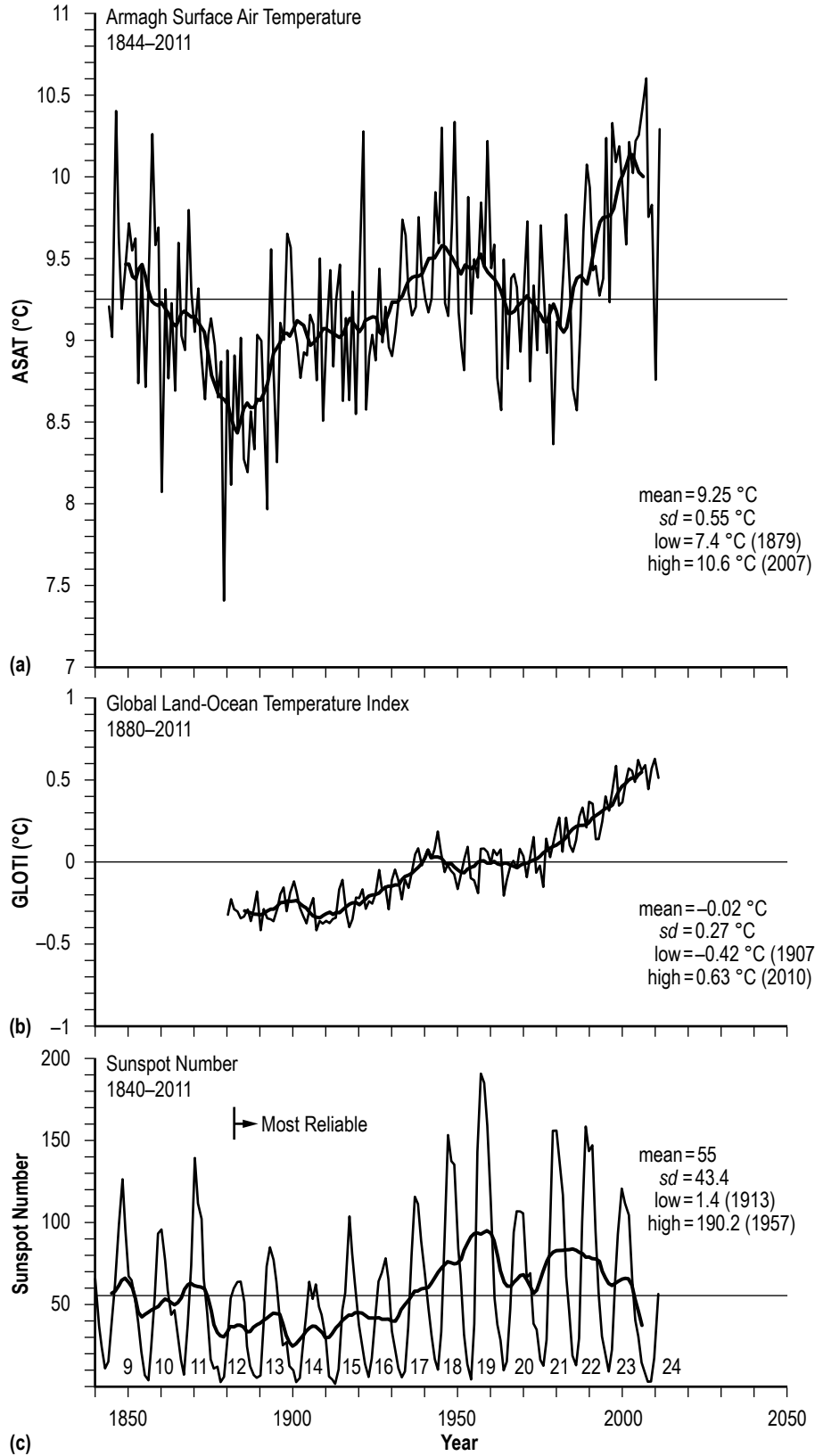


Figure 1. Annual (thin jagged line) and 10-yma (thick smoothed line) of (a) ASAT for the interval 1844–2011, (b) GLOTI for the interval 1880–2011, and (c) SSN for the interval 1840–2011.

The SSN is a measure of the strength of the solar activity, which varies over a period (or SC length) of about 10–12 years, based on annual or yearly averages of SSN during the modern era of sunspot observations (SC10–present). The SSN values shown in figure 1(c) correspond to the last 3 years of SC8 through the first 4 years of SC24, and the SSN data are available online at <ftp://ftp.ngdc.noaa.gov/STP/SOLAR\_DATA/SUNSPOT\_NUMBERS/INTERNATIONAL>.

The 10-yma values are shown to indicate trends in the annual values. For ASAT, its 10-yma value was lowest in 1883 (having a value of 8.44 °C) and highest in 2002 and 2003 (having a value of 10.13 °C). Hence, in terms of its 10-yma values, the ASAT has increased 1.69 °C in about 120 years, suggesting a rise in temperature at Armagh Observatory, Northern Ireland, at the average rate of about 0.014 °C per year or about 0.14 °C per decade (equivalent to a rise of about 0.025 °F per year or 0.25 °F per decade). It is interesting that prior to 1883, the 10-yma value at Armagh is found to have been trending downwards from a high of 9.46 °C in 1850 to the low of 8.44 °C in 1883, a decline of about 0.031 °C per year, or 0.31 °C per decade. Also interesting is that the rise in temperature from its low in 1883 rose quickly to 9.1 °C in 1901, leveled off for the next 35 years, rose once again to about 9.54 °C in 1945, and then fell to a local low of 9.05 °C in 1982 before rising once again to its highest observed peak temperature of 10.13 °C in 2002 and 2003.<sup>84</sup> Values since 2003 have fallen slightly to 10 °C (in 2011). The trend line, as determined using the 10-yma values, was below its long term mean between about 1857 and 1932 and again between about 1964 and 1984, while it was above its long term mean prior to 1857, between 1933 and 1963, and after 1984 (to the present).

For GLOTI, its 10-yma value was lowest in 1907 and 1908, measuring –0.34 °C, and highest in 2006, having a value of 0.55 °C. Hence, the GLOTI has increased 0.89 °C over about 103 years, indicating an average rise in warming of about 0.009 °C per year or 0.09 °C per decade (equivalent to an average rise of 0.016 °F per year or 0.16 °F per decade). Like the ASAT, it too shows a local peak (and flattening) in the early 1940s, followed by a rise after about 1967 to its observed peak in 2006, rising much faster over the past 40 years at an average rate of about 0.015 °C per year or 0.15 °C per decade. The trend line in the GLOTI was always below its long term mean prior to about 1940, while it was near its long term mean from about 1940–1970, and it has always been above its long term mean thereafter.

For SSN, its 10-yma values appear to have been trending downwards between about 1850 and 1900, rising slightly but remaining below its long term mean until about 1935, and then rapidly rising to its peak in the late 1950s (associated with SC19), staying above its long term mean from about 1935 until 2003.<sup>85–88</sup> The trend line is now below its long term mean and is expected to stay below it for the near term foreseeable future. While the trend line is currently below its long term mean, the annual SSN value rose above it in 2011 and will remain above it briefly, probably through about 2013–2015 since SC24 is now in its period of maximum phase, which typically lasts about 3–4 years in length.

Figure 2 shows the residuals for (a) ASAT and (b) GLOTI, where the residual is simply the difference between the observed annual value and the corresponding 10-yma value (i.e., for the same year). For ASAT, the mean is 0 °C and the *sd* is 0.41 °C. Hence, use of the 10-yma values reduces the variance by about 45%. Furthermore, runs-testing of the residuals yields a normal deviate of the sample  $z = 0.96$ , which by hypothesis testing suggests that the residuals are randomly distributed.<sup>89</sup> Therefore, use of the 10-yma values provides a convenient way to determine the overall yearly trend in the annual values of the ASAT.

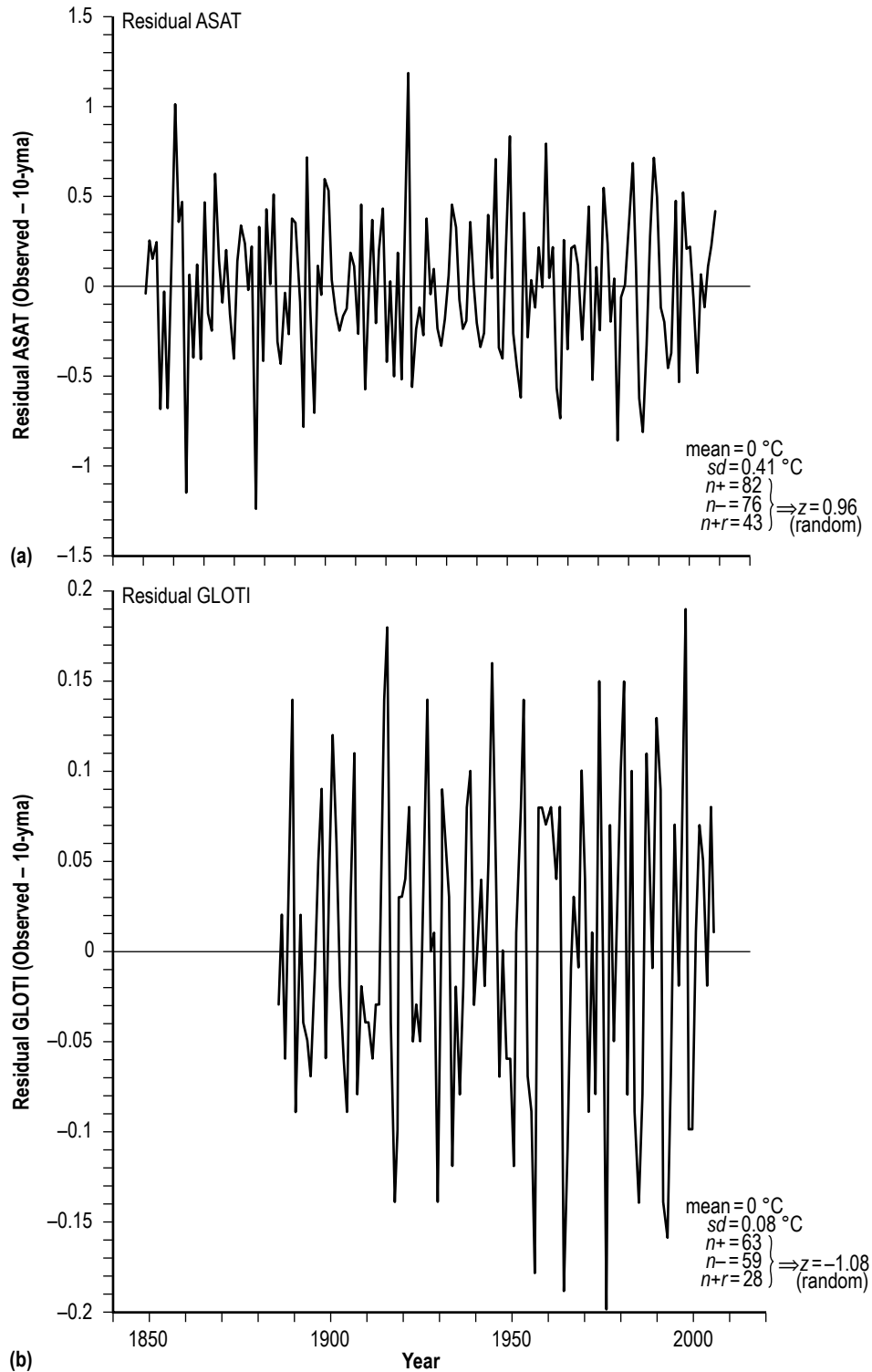


Figure 2. Residuals for (a) ASAT and (b) GLOTI, where the residual is simply the difference between the observed annual values and the corresponding 10-yma values (for the same year).

Similarly, for GLOTI, the mean is  $0\text{ }^{\circ}\text{C}$ , and the *sd* is  $0.08\text{ }^{\circ}\text{C}$ , yielding a reduction of the variance by about 90%. Runs-testing of its residuals also are found to be randomly distributed ( $z = -1.08$ ). Hence, as with the ASAT, the 10-yma values provide a convenient way to determine the overall yearly trend in the annual values of the GLOTI.

Figure 3 depicts the distributions of the residuals for (a) ASAT and (b) GLOTI. About 80% of the time, the 10-yma values for ASAT and GLOTI are within the interval  $0 \pm 0.5\text{ }^{\circ}\text{C}$  and  $0 \pm 0.1\text{ }^{\circ}\text{C}$ , respectively. Hence, given the annual values of ASAT and GLOTI, one can infer approximately their yearly 10-yma values (up to 5 years beyond the last available 10-yma value). For the year 2007 then, one expects the 10-yma value for ASAT to be about  $10.6 \pm 0.5\text{ }^{\circ}\text{C}$  and GLOTI to be about  $0.59 \pm 0.1\text{ }^{\circ}\text{C}$ , inferring only about a 10% chance that the 10-yma values will fall below  $10.1\text{ }^{\circ}\text{C}$  and  $0.49\text{ }^{\circ}\text{C}$ , respectively.

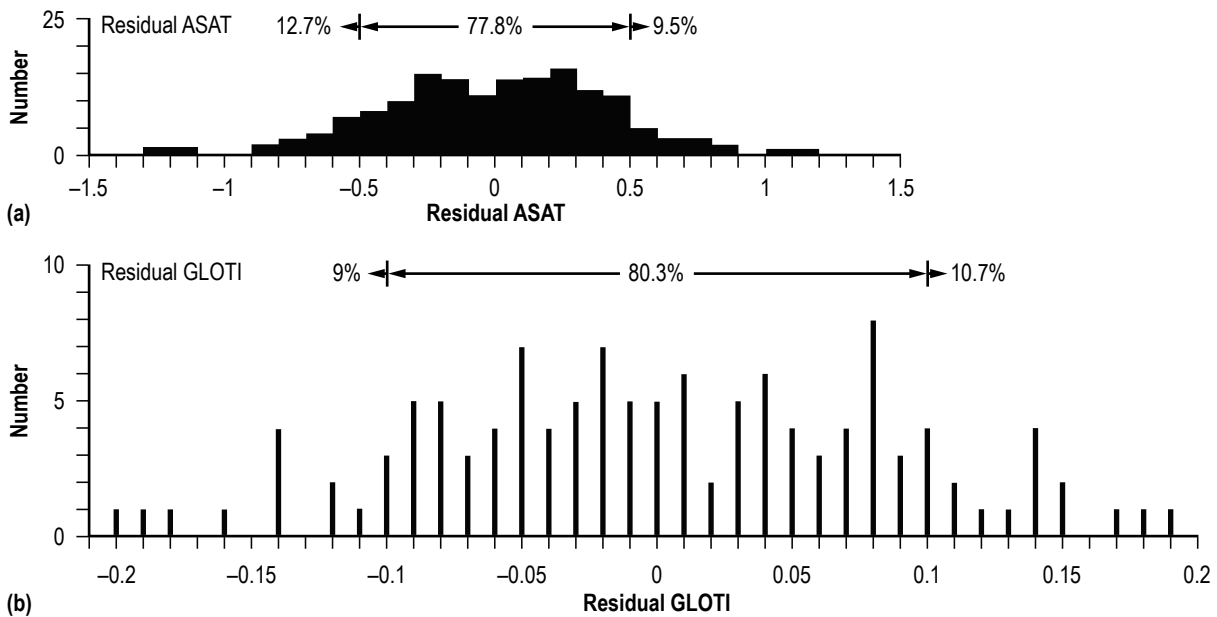


Figure 3. Distributions of the residuals for (a) ASAT and (b) GLOTI.

Figure 4(a) shows the scatter plot of the annual values of GLOTI versus ASAT for the interval 1880–2011. The thin vertical and horizontal lines represent the median values of the parameters, and the thick diagonal line represents the inferred preferential regression of GLOTI versus ASAT. Hence, as the annual value of the ASAT increases (decreases), one expects the annual value of the GLOTI to increase (decrease). The inferred regression is given by  $y = -2.822 + 0.302x$ , having a coefficient of linear correlation ( $r$ ) = 0.6 and coefficient of determination ( $r^2$ ) = 0.36, meaning that about 36% of the variance in the GLOTI annual values can be explained by the yearly variation in the ASAT annual values (or vice versa) during the interval 1880–2011. The inferred regression has a standard error of estimate (*se*) of  $0.22\text{ }^{\circ}\text{C}$ , and hypothesis testing of the slope reveals that the inferred regression is statistically important at confidence level (*cl*) > 99.9%. Also shown in figure 4(a) is the result of Fisher’s exact test for the observed  $2 \times 2$  contingency table (and for any other result that shows

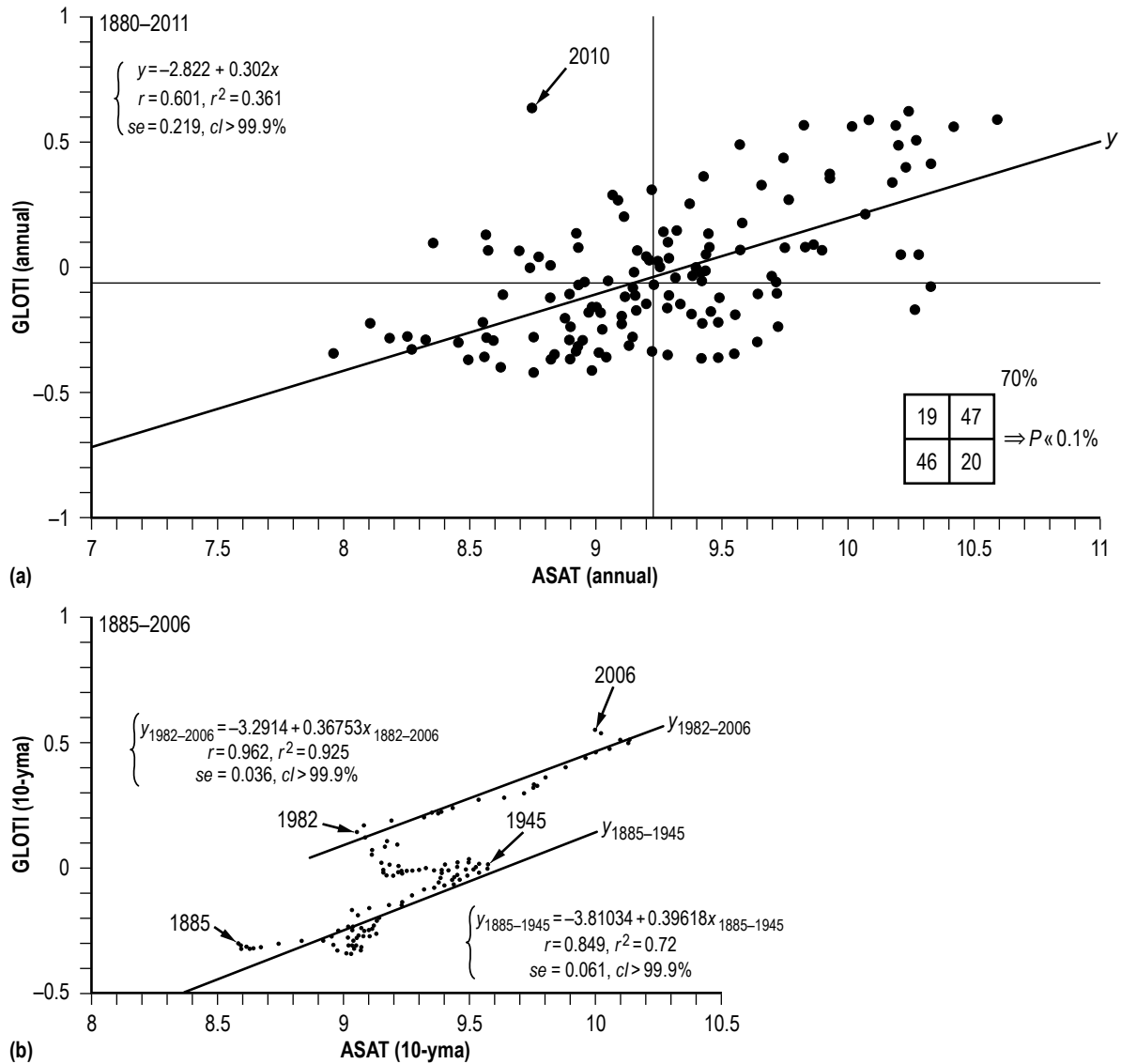


Figure 4. Scatter plots of (a) annual values of GLOTI versus ASAT for the interval 1880–2011 and (b) GLOTI versus ASAT using 10-yma values for the interval 1885–2006.

a greater departure from independence<sup>90</sup>) being the probability ( $P$ )  $\ll 0.1\%$ . Hence, there is strong statistical evidence linking ASAT and GLOTI, with about 70% (= 93/132) of the annual values obeying the paradigm of warmer (cooler) values of GLOTI being associated with warmer (cooler) values of ASAT.

However, a peculiarity is noticeable in figure 4(a); in particular, the annual values for the year 2010. For GLOTI, the annual value for 2010 measures 0.63 °C, the warmest index value on record; while for ASAT, the annual value for 2010 measures only 8.75 °C, the coolest temperature measured at Armagh since 1986. For the first four months of the year 2010, the Oceanic Niño Index (ONI) indicated the presence of a weakening El Niño (EN), followed by two months of neutral



conditions and then a strengthening La Niña (LN) for the remainder of the year. In contrast, ONI for the year 1986 displayed neutral conditions for the first seven months of the year followed by a strengthening EN for the remainder of the year (ONI monthly anomalies are available online at <[http://www.cpc.ncep.noaa.gov/products/analysis\\_monitoring/ensostuff/ensoyears.shtml](http://www.cpc.ncep.noaa.gov/products/analysis_monitoring/ensostuff/ensoyears.shtml)>). So, it is somewhat puzzling as to why such a large discrepancy exists between the inferred GLOTI and the observed GLOTI for the year 2010 given the observed ASAT. The discrepancy measures 3.7 *se* based on the inferred, highly statistically important positive preferential regression determined for GLOTI versus ASAT.

Figure 4(b) displays the scatter plot of GLOTI versus ASAT using 10-yma values. The scatter plot strangely suggests two different regimes of regression fits: one fit active for the interval 1885–1945 and the other fit active from about 1982–2006 (the year of the last available 10-yma values used in this TP), with a transition occurring between them. Both regressions are inferred to be statistically important, with the regression for the current interval having  $r = 0.962$ ,  $r^2 = 0.925$ ,  $se = 0.036$  °C, and  $cl > 99.9\%$ . While true, the observed 10-yma value of GLOTI for 2006 (0.55 °C) is about 0.1 °C warmer than that found using the inferred regression for 1982–2006, and it is about 0.4 °C warmer than that found using the 1885–1945 regression given the 10-yma value of ASAT for 2006 (10 °C). One can only speculate as to why there exists this observed discrepancy represented by two statistically important inferred regressions with a transition occurring between them. For example, are the discrepancies due to the increased concentration of anthropogenic gases in the Earth’s atmosphere, thereby altering the relationship between GLOTI and ASAT; or are the discrepancies somehow related to the changing phase of the Atlantic Multidecadal Oscillation (AMO); or are the discrepancies due to some unknown problems with one or both of the indices; or are the discrepancies due to some unknown combination of nonlinear effects; or etc.?

Figure 5 shows the variation in first difference (*fd*) values of the 10-yma values for (a) ASAT and (b) GLOTI, where the *fd* is defined as the difference between the 10-yma value for year (*t*) + 1 minus the 10-yma value for year *t*, and figure 6 shows the distribution of the *fd* values for (a) ASAT and (b) GLOTI. For ASAT, its *fd* values have a mean = 0 °C and  $sd = 0.05$  °C, with the interval  $fd = 0 \pm 0.05$  °C capturing about 73% of the *fd* values. For GLOTI, its *fd* values have a mean = 0.01 °C and  $sd = 0.01$  °C, with the interval  $fd = 0.01 \pm 0.01$  °C capturing about 74% of the *fd* values. Hence, using the mean and *sd* in the *fd* values allows one to approximate the next yearly 10-yma value (i.e., for 2007).



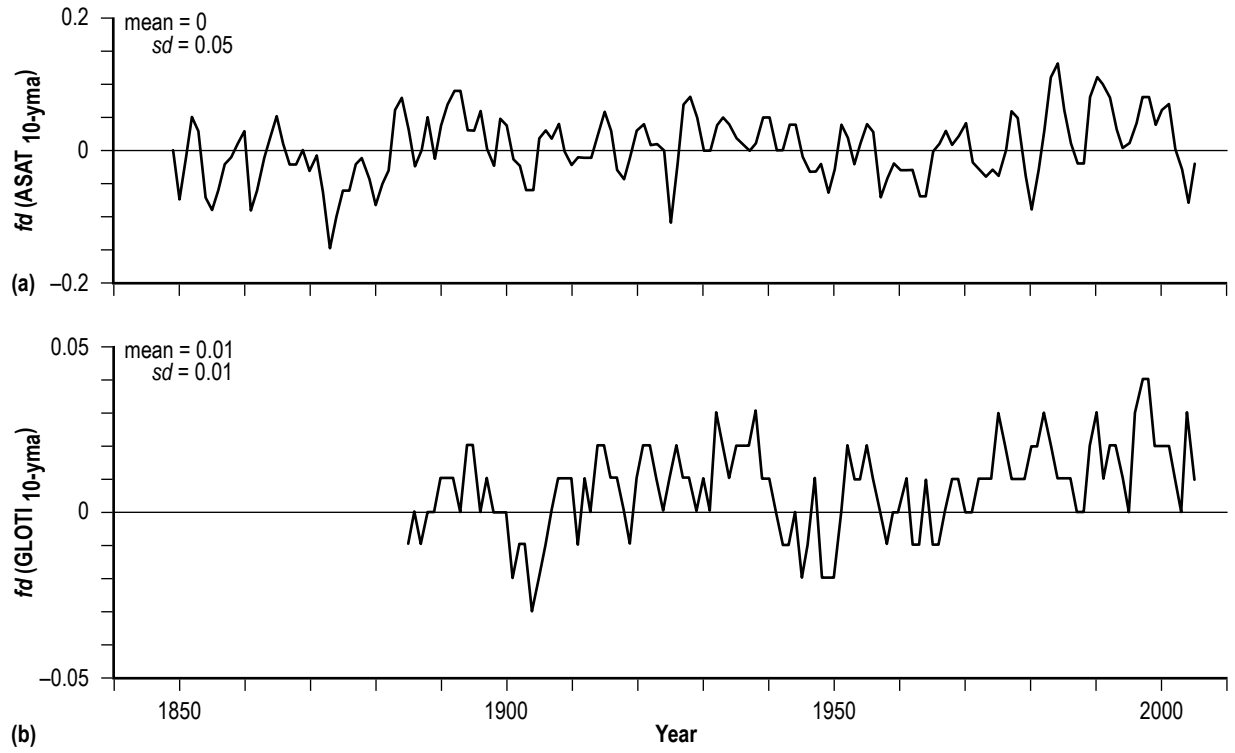


Figure 5. Variation in  $fd$  values of the 10-yma values for (a) ASAT and (b) GLOTI.

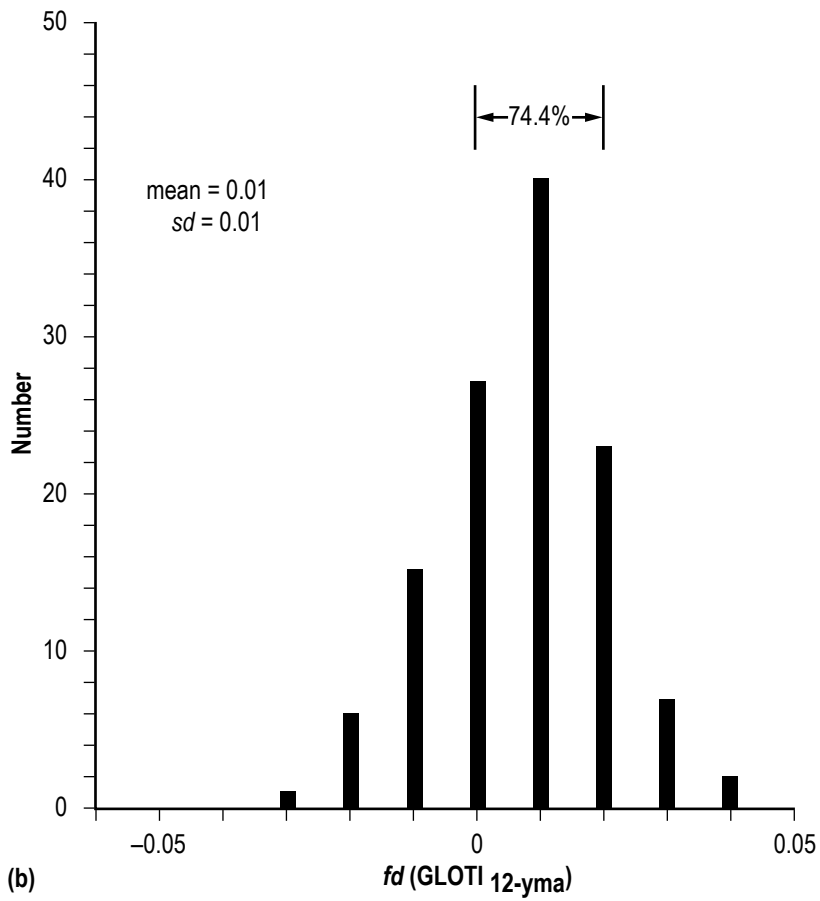
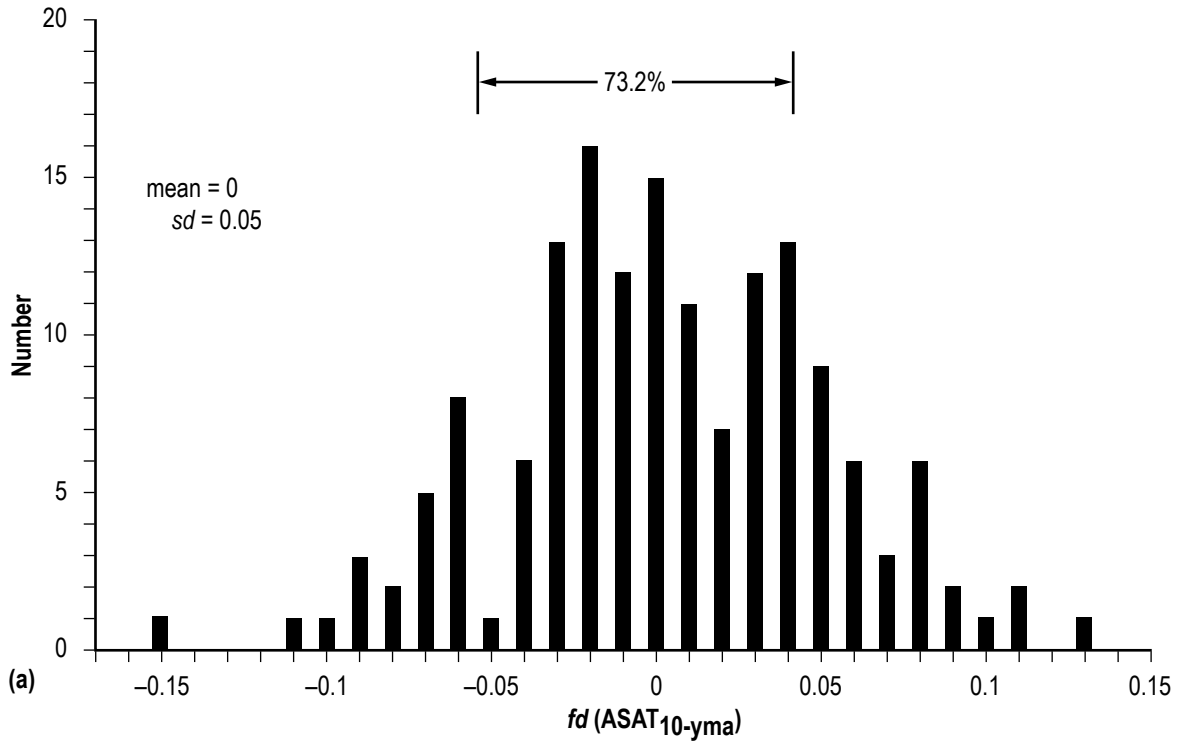


Figure 6. Distribution of the  $fd$  values for (a) ASAT and (b) GLOTI.

For ASAT, its 10-yma value for 2006 measured  $10\text{ }^{\circ}\text{C}$ , inferring that its 10-yma value for 2007 should be about  $10+0\pm 0.05\text{ }^{\circ}\text{C}$ , or  $10\pm 0.05\text{ }^{\circ}\text{C}$ , presuming that the *fd* value for 2007 falls within the mean  $\pm 1\text{ }sd$  prediction interval (a value slightly lower than that deduced using the yearly residuals (see fig. 3 discussion). Using this value, one estimates the annual ASAT for the year 2012 to be about  $9.58\pm 1\text{ }^{\circ}\text{C}$ , or below  $10.58\text{ }^{\circ}\text{C}$ . It measured  $10.28\text{ }^{\circ}\text{C}$  in 2011, and the January–September 2012 ASAT average is about  $10.7\text{ }^{\circ}\text{C}$ . (Now that the year 2012 is complete, ASAT for the year is known to be  $9.7\text{ }^{\circ}\text{C}$ .)

For GLOTI, its 10-yma value for 2006 measured  $0.55\text{ }^{\circ}\text{C}$ , inferring that its 10-yma value for 2007 should be about  $0.55+0.01\pm 0.01\text{ }^{\circ}\text{C}$  or  $0.56\pm 0.01\text{ }^{\circ}\text{C}$ . Using this value, one estimates the annual value of GLOTI for the year 2012 to be about  $0.69\pm 0.2\text{ }^{\circ}\text{C}$ , or below  $0.89\text{ }^{\circ}\text{C}$ . The warmest GLOTI to date is  $0.63\text{ }^{\circ}\text{C}$  in 2010. The GLOTI measured  $0.51\text{ }^{\circ}\text{C}$  in 2011, and the January–September 2012 GLOTI average is about  $0.5\text{ }^{\circ}\text{C}$ . Because ONI presently is showing signs of a slight warming (being  $0.6\text{ }^{\circ}\text{C}$  in October), perhaps suggesting the possible start of an EN event in late 2012, one expects the GLOTI for the year 2012 to be  $>0.5\text{ }^{\circ}\text{C}$ . (Again, now that the year 2012 is complete, GLOTI for the year is known to be  $0.56\text{ }^{\circ}\text{C}$ .)

## 2.2 ASC, PER, Rmax, <SSN>, <ASAT> and <GLOTI> for SC10–SC23

Figure 7 shows the variation of both the actual cyclic mean value (the thin dotted line) and the two-cycle moving average (the thick smoothed line for SC10–SC23 of (a) ascent duration (ASC) (i.e., the ascent period, defined herein as the elapsed time from sunspot Rmin year to sunspot Rmax year in the same cycle, based on annual averages of SSN), (b) the period (PER) (i.e., the SC length, or period, defined herein as the elapsed time between two consecutive sunspot minima years based on annual averages of SSN), (c) Rmax (i.e., the maximum amplitude, or maximum yearly value of SSN, for an SC), (d) <SSN> (i.e., the average SSN over the SC, from sunspot minimum year to the following sunspot minimum year), (e) <ASAT> (i.e., the average ASAT over the SC, from sunspot minimum year to the following sunspot minimum year), and (f) <GLOTI> (i.e., the average GLOTI over the SC from sunspot minimum year to the following sunspot minimum year). The use of the symbols <> simply indicates that the computed values are averages of the yearly parametric values over each SC (from sunspot minimum year to sunspot minimum year).

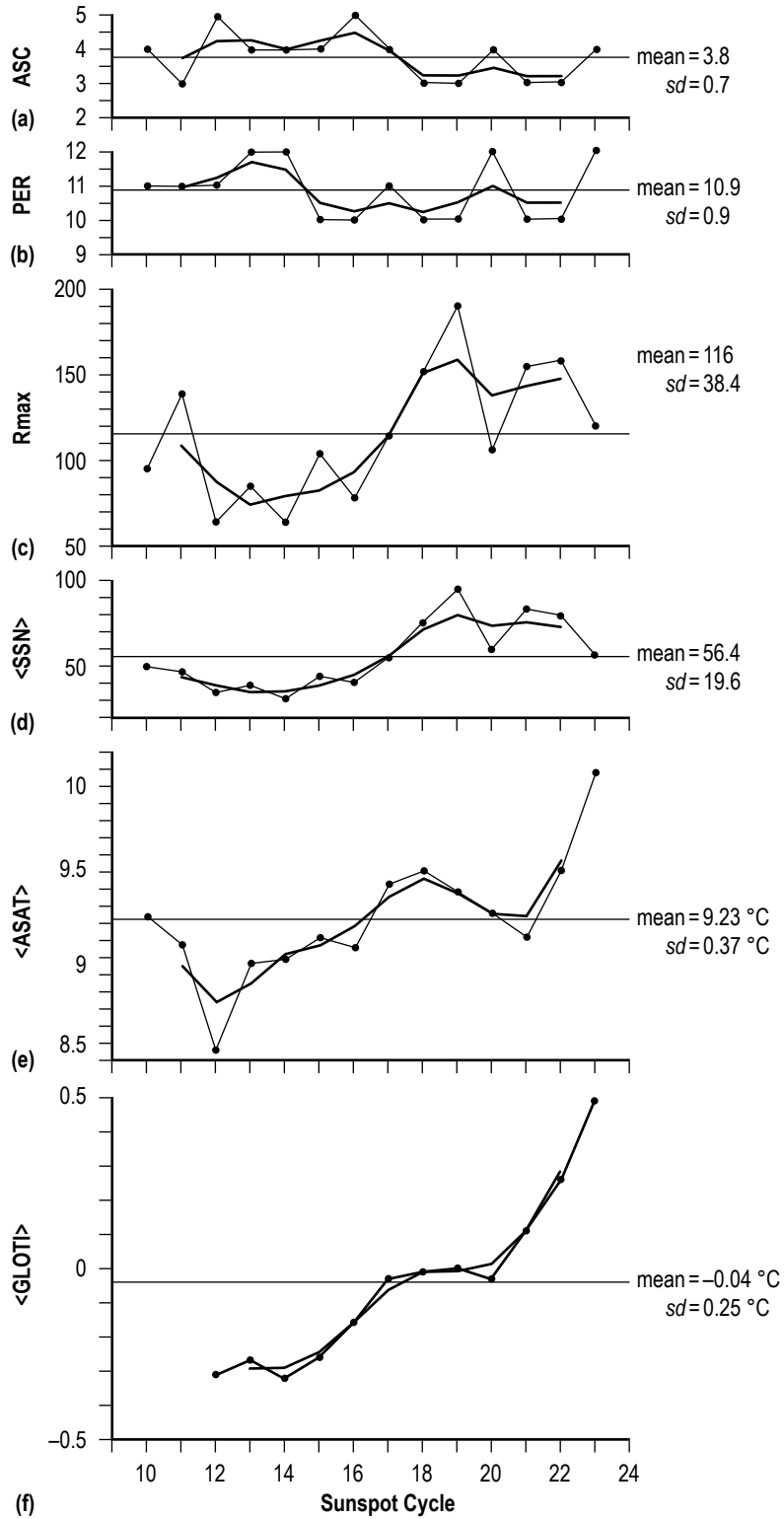


Figure 7. Variation of both the actual cyclic value (the thin dotted line) and the two-cycle moving average (the thick smoothed line) for SC10–SC23 of (a) ASC, (b) PER, (c) Rmax, (d) <SSN>, (e) <ASAT>, and (f) <GLOTI>.

On the basis of yearly SSN, the modern era of SCs is found to have ASC periods averaging about  $3.8 \pm 0.7$  years (i.e., the mean  $\pm 1$  *sd* interval), ranging incrementally 3 to 5 years in length. Cycles with ASC = 3 years are considered fast risers, while those with ASC = 4 years are considered average risers, and those with ASC = 5 years are considered slow risers. For the modern era, there have been five SCs classified as fast risers, including SC11, SC18, SC19, SC21, and SC22; seven cycles classified as average risers, including SC10, SC13–SC15, SC17, SC20, and SC23; and only two cycles classified as slow risers, including SC12 and SC16. SC24, the current ongoing SC, had its Rmin in terms of annual SSN in the year 2008 and is presently in its fifth year of rise (2013). Presuming SC24 is not a statistical outlier, one expects that its maximum annual amplitude will occur in either 2012 or 2013 and that SC24 will be classified as a slow riser. (SSN measured 57.5 in 2012. Through May 2013, SSN averages 62.)

Concerning PER, its mean + 1 *sd* interval is computed to be  $10.9 \pm 0.9$  years based on annual averages of SSN, ranging incrementally 10 to 12 years. Cycles with PER = 10 years are considered short-period cycles (they include SC15, SC16, SC18, SC19, SC21, and SC22), those having PER = 11 years are considered average-period cycles (they include SC10–SC12, and SC17), and those having PER = 12 years are considered long-period cycles (they include SC13, SC14, SC20, and SC23). Presuming SC24 is not a statistical outlier, one expects SC24 to end before the year 2020 (i.e., in 2017 if it is a short-period cycle, in 2018 if it is an average-period cycle, or in 2019 if it is a long-period cycle). During the modern era, there has never been an SC having PER >12 years based on annual averages of SSN; so, if SC24 continues through 2020 or later, it would be a statistical outlier with respect to the 14 cycles comprising the modern era of SCs. (Based on the 12-month moving average of monthly mean SSN (also called smoothed monthly mean SSN), SC lengths are found to span 116 months for SC22 to 151 months for SC23.)<sup>91–93</sup>

Concerning Rmax, its mean + 1 *sd* interval is computed to be  $116 \pm 38.4$ , based on annual averages of SSN. Cycles having Rmax  $\geq 116$  include SC11 and SC18–SC23, while cycles having Rmax <116 include SC10–SC17 and SC20. If, instead of using the mean Rmax, one chose to sort the cycles using the median Rmax value, then SC17 would be grouped with the larger Rmax group. The largest Rmax is 190.2 (measured for SC19), and the smallest Rmax is 63.5 (measured for SC14; SC12 had Rmax = 63.7). SC24 is expected to have Rmax <116, probably near Rmax = 70.<sup>94–97</sup>

Concerning <SSN>, its mean + 1 *sd* interval is computed to be  $56.4 \pm 19.6$  based on annual averages of SSN for each SC. Cycles having <SSN>  $\geq 56.4$  include SC18–SC23, while cycles having <SSN> <56.4 include SC10–SC17. Again, if instead of using the mean <SSN> as the discriminator for groupings of <SSN>, one chose to use the median <SSN> value, then SC17 would be grouped with the larger <SSN> group. Because of the strong behavioral similarity between <SSN> and Rmax (see below), one expects <SSN> to be <56.4 for SC24.

Concerning <ASAT>, its mean + 1 *sd* interval is computed to be  $9.23 \pm 0.37$  °C. Cycles having <ASAT>  $\geq 9.23$  °C include SC10 and SC17–SC23, while cycles having <ASAT> <9.23 °C include SC11–SC16 and SC21. SC23 (spanning 1996–2007), having <ASAT> = 10.08 °C, has the warmest <ASAT> of any modern era SC, being about 2.3 *sd* warmer than the mean. In contrast, SC12 (spanning 1878–1888), having <ASAT> = 8.46 °C, has the coolest <ASAT> on record, being about 2.1 *sd* cooler than the mean. Based on the average observed change in <ASAT> between two consecutive

cycles, one estimates that  $\langle \text{ASAT} \rangle$  for SC24 likely will be about  $10.08 + 0.06 \pm 0.33$  °C, or about  $10.14 \pm 0.33$  °C (i.e.,  $\langle \text{ASAT} \rangle$  is expected to be  $<10.47$  °C for SC24; any  $\langle \text{ASAT} \rangle$  value warmer than  $10.08$  °C would be a new record high value).

Concerning  $\langle \text{GLOTI} \rangle$ , its mean + 1 *sd* interval is computed to be  $-0.04 \pm 0.25$  °C. Cycles having  $\langle \text{GLOTI} \rangle \geq -0.04$  °C (i.e., warmer than  $-0.04$  °C) include SC17–SC23, while cycles having  $\langle \text{GLOTI} \rangle < -0.04$  °C (i.e., cooler than  $-0.04$  °C) include SC12–SC16. SC23, having  $\langle \text{GLOTI} \rangle = 0.49$  °C, has the warmest  $\langle \text{GLOTI} \rangle$  on record, being about 2.1 *sd* warmer than the mean. In contrast, SC14 (spanning 1901–1912), having  $\langle \text{GLOTI} \rangle = -0.32$  °C, has the coolest  $\langle \text{GLOTI} \rangle$  on record, being about 1.1 *sd* cooler than the mean. Based on the average observed change in  $\langle \text{GLOTI} \rangle$  between two consecutive cycles, one estimates that  $\langle \text{GLOTI} \rangle$  for SC24 likely will be about  $0.49 + 0.07 \pm 0.09$  °C, or about  $0.56 \pm 0.09$  °C (i.e.,  $\langle \text{GLOTI} \rangle < 0.65$  °C for SC24, and any  $\langle \text{GLOTI} \rangle$  value warmer than  $0.49$  °C would be a new record high value).

Based on the two-cycle moving average (shown to reflect the variation as related to the Hale cycle<sup>98</sup>), it seems very likely that ASC, PER,  $\langle \text{ASAT} \rangle$ , and  $\langle \text{GLOTI} \rangle$  will trend upwards for SC23, while Rmax and  $\langle \text{SSN} \rangle$  will trend downwards. In other words, it now seems quite clear that  $\langle \text{ASAT} \rangle$  and  $\langle \text{GLOTI} \rangle$  will no longer consistently track the trend in solar activity (i.e., Rmax or  $\langle \text{SSN} \rangle$ ), as they appear to have done prior to about SC21. (There has been consistent warming since SC21, although solar activity has been in decline, thus indicating a lessening in solar forcing on climate.)<sup>99–101</sup>

Regarding the grouping of SCs as fast risers, average risers, slow risers, short-period cycles, average-period cycles, and long-period cycles, one computes the following means and *sds*:

(1) Fast risers (ASC = 3 years) have PER =  $10.2 \pm 0.45$  years (the mean  $\pm 1$  *sd* prediction interval), Rmax =  $158.8 \pm 19$ ,  $\langle \text{SSN} \rangle = 75.9 \pm 17.5$ ,  $\langle \text{ASAT} \rangle = 9.32 \pm 0.21$  °C, and  $\langle \text{GLOTI} \rangle = 0.09 \pm 0.13$  °C.

(2) Average risers (ASC = 4 years) have PER =  $11.43 \pm 0.79$  years, Rmax =  $98.3 \pm 19.1$ ,  $\langle \text{SSN} \rangle = 47.7 \pm 10.2$ ,  $\langle \text{ASAT} \rangle = 9.3 \pm 0.38$  °C, and  $\langle \text{GLOTI} \rangle = -0.07 \pm 0.3$  °C.

(3) Slow risers (ASC = 5 years) have PER =  $10.5 \pm 0.71$  years, Rmax =  $70.8 \pm 10$ ,  $\langle \text{SSN} \rangle = 37.8 \pm 4.5$ ,  $\langle \text{ASAT} \rangle = 8.76 \pm 0.42$  °C, and  $\langle \text{GLOTI} \rangle = -0.24 \pm 0.11$  °C.

(4) Short-period cycles have ASC =  $3.5 \pm 0.84$  years, Rmax =  $139.4 \pm 40.9$ ,  $\langle \text{SSN} \rangle = 69.6 \pm 21.9$ ,  $\langle \text{ASAT} \rangle = 9.29 \pm 0.21$  °C, and  $\langle \text{GLOTI} \rangle = -0.01 \pm 0.19$  °C.

(5) Average-period cycles have ASC =  $4 \pm 0.82$  years, Rmax =  $103.2 \pm 31.7$ ,  $\langle \text{SSN} \rangle = 46.7 \pm 8.7$ ,  $\langle \text{ASAT} \rangle = 9.05 \pm 0.42$  °C, and  $\langle \text{GLOTI} \rangle = -0.17 \pm 0.2$  °C.

(6) Long-period cycles have ASC =  $4 \pm 0$  years, Rmax =  $93.5 \pm 24.5$ ,  $\langle \text{SSN} \rangle = 46.3 \pm 13.5$ ,  $\langle \text{ASAT} \rangle = 9.33 \pm 0.52$  °C, and  $\langle \text{GLOTI} \rangle = -0.03 \pm 0.37$  °C.

Hence, fast risers tend to have higher  $R_{\max}$ ,  $\langle \text{SSN} \rangle$ , and  $\langle \text{GLOTI} \rangle$  as compared to average or slow risers, and short-period cycles tend to have higher  $R_{\max}$  and  $\langle \text{SSN} \rangle$  as compared to average- or long-period cycles. Higher or lower values of  $\langle \text{ASAT} \rangle$  do not appear to differentiate between ASC or PER classes (in particular, fast versus slow riser or short- versus long-period cycles), based on the  $t$  statistic for independent samples, used for comparing two means from independent samples.<sup>89</sup> Likewise, higher or lower values of  $\langle \text{GLOTI} \rangle$  do not appear to differentiate between PER classes of SCs. (Presently, SC24 is believed to be a slow riser of possibly long-period; hence, one expects it to have  $R_{\max}$  and  $\langle \text{SSN} \rangle$  below respective long term means, peaking in 2012 or 2013 and ending in 2019 or later, in terms of annual averages of SSN.)

In their analysis, Solheim et al.<sup>61</sup> used SC lengths determined differently than that used here, which is one based on the use of annual yearly averages of SSN. Depending upon the parameter used to determine SC length, whether it is the number of sunspot groups, the number of spotless days, sunspot area, the ratio of new cycle to old cycle sunspots, curve fitting, etc., any number of different SC lengths can be determined, and those lengths can vary by several months or more.<sup>102,103</sup> Using annual averages simplifies the issue of determining SC length (i.e., based on annual averages of SSN, a cycle length is determined to be of integer length, 10 years, 11 years, 12 years, etc.).

As previously noted, Solheim et al. reported no strong association between the length of the SC and the temperature over that same SC (as also can be gleaned above using SC lengths determined from annual averages of SSN (i.e., the mean temperature and associated  $sd$  for short-, average-, and long-period SC classes)).<sup>61</sup> Additionally, they reported that SCs of shorter (longer) length were strongly associated with warmer (cooler) temperatures during the following SC. Based on SC lengths determined using annual averages of SSN, one finds a similar result, although the result is found not to be statistically important based on the  $t$  statistic for independent samples, neither for  $\langle \text{ASAT} \rangle$  nor  $\langle \text{GLOTI} \rangle$ . For example, short-period cycles (PER = 10 years) are found to have  $\langle \text{ASAT} \rangle = 9.46 \pm 0.34$  °C and  $\langle \text{GLOTI} \rangle = 0.11 \pm 0.22$  °C during the following SC, while average-period cycles (PER = 11 years) have  $\langle \text{ASAT} \rangle = 9 \pm 0.43$  °C and  $\langle \text{GLOTI} \rangle = -0.2 \pm 0.16$  °C, and long-period cycles (PER = 12 years) have  $\langle \text{ASAT} \rangle = 9.08 \pm 0.08$  °C and  $\langle \text{GLOTI} \rangle = -0.16 \pm 0.23$  °C during the following SC. So, while shorter (longer) period cycles appear to be followed by warmer (cooler) temperature, based on the means and  $sd$  of the temperatures, the differences do not appear to be statistically meaningful ( $t = 1.8$  for  $\langle \text{ASAT} \rangle$  and  $t = 1.7$  for  $\langle \text{GLOTI} \rangle$  based on the six short-period cycles and three long-period cycles of the modern era, inferring  $cl < 90\%$ ).

Figure 8 shows the scatter plots of the cyclic averages of (a)  $\langle \text{ASAT} \rangle$  versus  $R_{\max}$ , (b)  $\langle \text{GLOTI} \rangle$  versus  $R_{\max}$ , (c)  $\langle \text{ASAT} \rangle$  versus  $\langle \text{SSN} \rangle$ , and (d)  $\langle \text{GLOTI} \rangle$  versus  $\langle \text{SSN} \rangle$ , where the numbered filled circles refer to the SC number. In each subpanel, the vertical and horizontal lines indicate the median values, and the diagonal line, inferring a direct preferential correlation (i.e., an increase or decrease in  $y$  being associated with an increase or decrease in  $x$ ), indicates the inferred regression fit between the  $y$  and  $x$  parameters. Also given in each subpanel are the inferred regression equations  $y$ ,  $r$ ,  $r^2$ ,  $se$ ,  $cl$ , and  $P$ , where  $y$  refers to the inferred regression equation,  $r$  to the coefficient of linear correlation,  $r^2$  to the coefficient of determination (a measure of the amount of variance explained by the inferred regression),  $se$  to the standard error of estimate,  $cl$  to the confidence level, and  $P$  to the probability of occurrence by chance based on the Fisher's exact test for  $2 \times 2$  contingency tables.

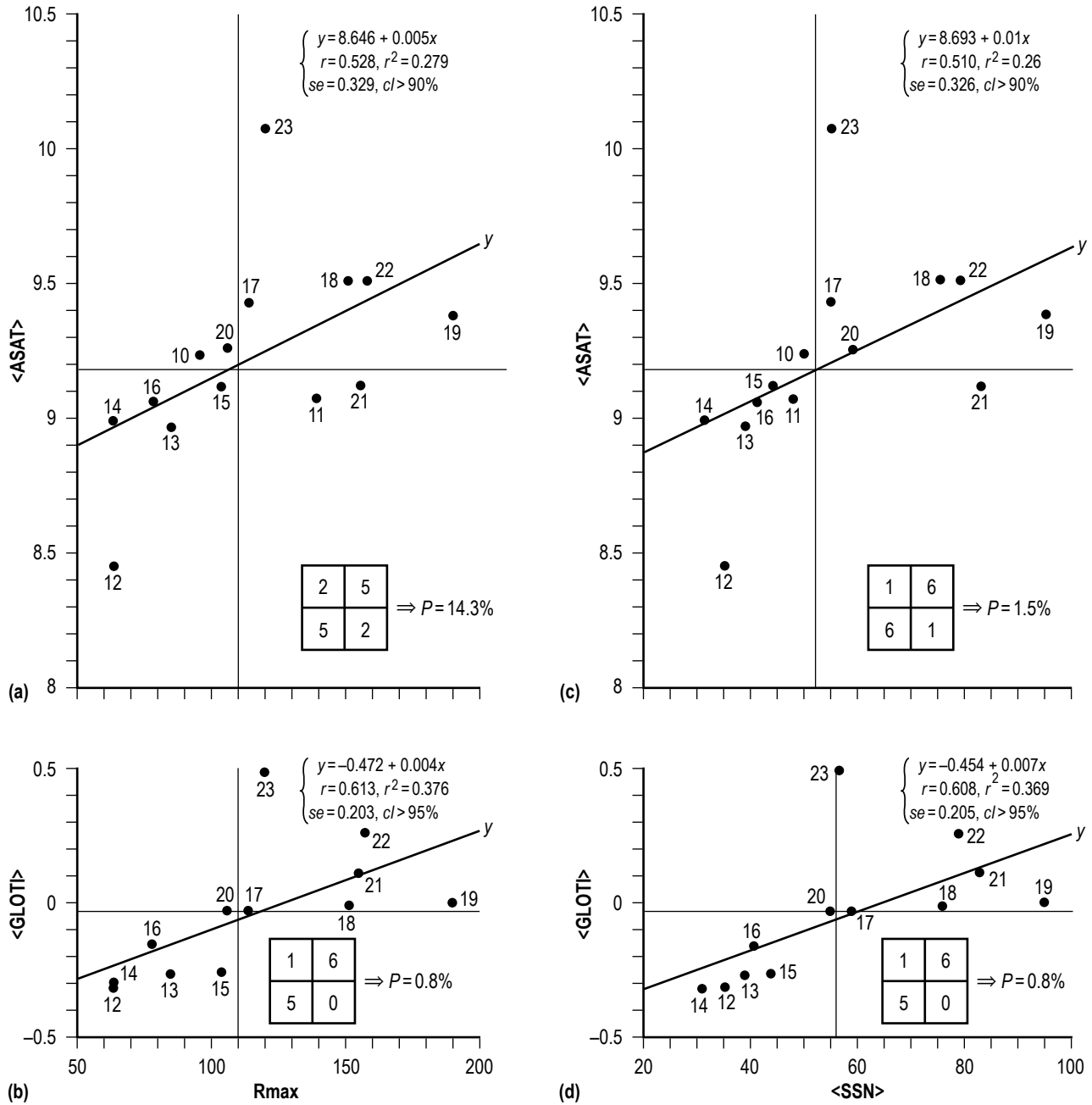


Figure 8. Scatter plots of the cyclic averages of (a)  $\langle \text{ASAT} \rangle$  versus  $R_{\text{max}}$ , (b)  $\langle \text{GLOTI} \rangle$  versus  $R_{\text{max}}$ , (c)  $\langle \text{ASAT} \rangle$  versus  $\langle \text{SSN} \rangle$ , and (d)  $\langle \text{GLOTI} \rangle$  versus  $\langle \text{SSN} \rangle$ , where the numbered filled-circles refer to the SC.

Concerning the inferred correlation between  $\langle \text{ASAT} \rangle$  and  $R_{\text{max}}$ , the regression is found to be only of marginal statistical importance ( $cl > 90\%$ ), having  $r = 0.53$ . Based on Fisher's exact test for  $2 \times 2$  contingency tables, the probability of obtaining the observed result, or one more suggestive of a departure from independence, is computed to be  $P = 14.3\%$ . Therefore, the association of  $\langle \text{ASAT} \rangle$  against  $R_{\text{max}}$  must be considered weak. Since  $R_{\text{max}}$  for SC24 is anticipated to be less than the



median value, there appears to be only about a 30% chance that SC24 will have <ASAT> larger than its median based on its expected Rmax alone (from the 2×2 contingency table).

Concerning the inferred correlation between <GLOTI> and Rmax, the regression is found to be statistically important ( $cl > 95\%$ ), having  $r = 0.61$ . Also, based on Fisher's exact test for 2×2 contingency tables, the association of <GLOTI> against Rmax is found to be considerably stronger, having  $P = 0.8\%$  (i.e., the probability of obtaining the observed result or one more suggestive of a departure from independence is  $< 1\%$ ). Hence, given that SC24 is expected to have an Rmax less than the median value, one expects <GLOTI> for SC24 very probably to be less than its median value, again based on Rmax alone.

Concerning the inferred correlation between <ASAT> and <SSN>, the regression is found to be only of marginal statistical importance ( $cl > 90\%$ ), having  $r = 0.51$ . However, based on Fisher's exact test for 2×2 contingency tables, the probability of obtaining the observed result, or one more suggestive of a departure from independence, is computed to be  $P = 1.5\%$ . Hence, presuming that SC24 will have <SSN> less than its median value, one expects <ASAT> for SC24 likewise to be less than its median value based on <SSN> alone.

Lastly, concerning the inferred correlation between <GLOTI> and <SSN>, the regression is found to be statistically important ( $cl > 95\%$ ), having  $r = 0.61$ . Also, based on Fisher's exact test for 2×2 contingency tables, the association of <GLOTI> against <SSN> is found to be considerably stronger, having  $P = 0.8\%$ . Hence, given that SC24 is expected to have <SSN> less than the median value, one expects <GLOTI> for SC24 very likely to be less than its median value based on <SSN> alone.

However, the locations of SC12 and SC23 (the coolest and warmest <ASAT> values, respectively) in the scatter plots involving <ASAT> are troubling. Based on figure 8(a), SC12 has an <ASAT> value about 1.5 *se* below the inferred regression value, while SC23 has an <ASAT> value about 2.5 *se* above the inferred regression value. Based on figure 8(b), SC12 has an <ASAT> value about 1.8 *se* below the inferred regression value, while SC23 has an <ASAT> value about 2.5 *se* above the inferred regression value.

Likewise, while SC12 has <GLOTI> values close to its inferred values (given Rmax and <SSN>), the <GLOTI> values for SC23 are considerably above them (given its Rmax and <SSN>), being about 2.4 *se* above its inferred regression value based on Rmax and 2.7 *se* above its inferred regression value based on <SSN>. Therefore, something other than the Rmax or average SSN over the cycle appears to be driving the increased temperature anomaly as measured using <GLOTI>.

Figure 9 displays the scatter plots of (a) <GLOTI> versus <ASAT> and (b) <SSN> versus Rmax. Both scatter plots are found to be highly statistically important ( $cl > 99.9\%$ ), with the former relation having  $r = 0.86$  and the latter relation having  $r = 0.94$ . Based on Fisher's exact test,  $P = 0.8\%$  for the former relation and  $P = 1.5\%$  for the latter relation. Hence, when <ASAT> is above (below) its median value, one strongly expects <GLOTI> to be above (below) its median value. Similarly, when Rmax is above (below) its median value, one clearly expects <SSN> to be above (below) its median value.

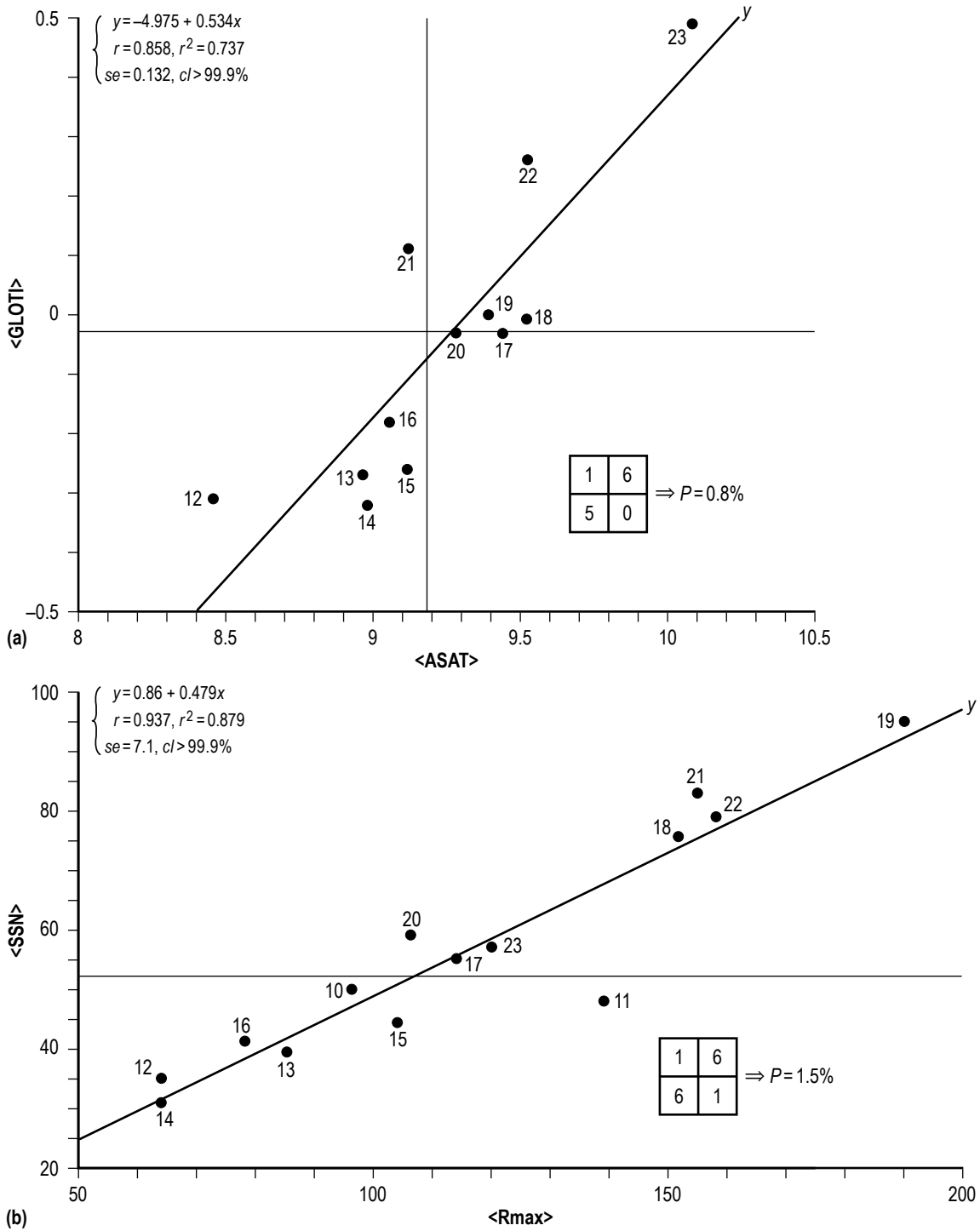


Figure 9. Scatter plots of (a)  $\langle \text{GLOTI} \rangle$  versus  $\langle \text{ASAT} \rangle$  and (b)  $\langle \text{SSN} \rangle$  versus  $\text{Rmax}$ .

Figure 10 shows the variation of (a) SSN, (b) ASAT, and (c) GLOTI from January 1996–September 2012, as well as the variation of (d)  $\langle \text{SSN} \rangle$ , (e)  $\langle \text{ASAT} \rangle$ , and (f)  $\langle \text{GLOTI} \rangle$  for elapsed time in years past the sunspot minimum year for SC23 (the unfilled histograms) and SC24 (the filled

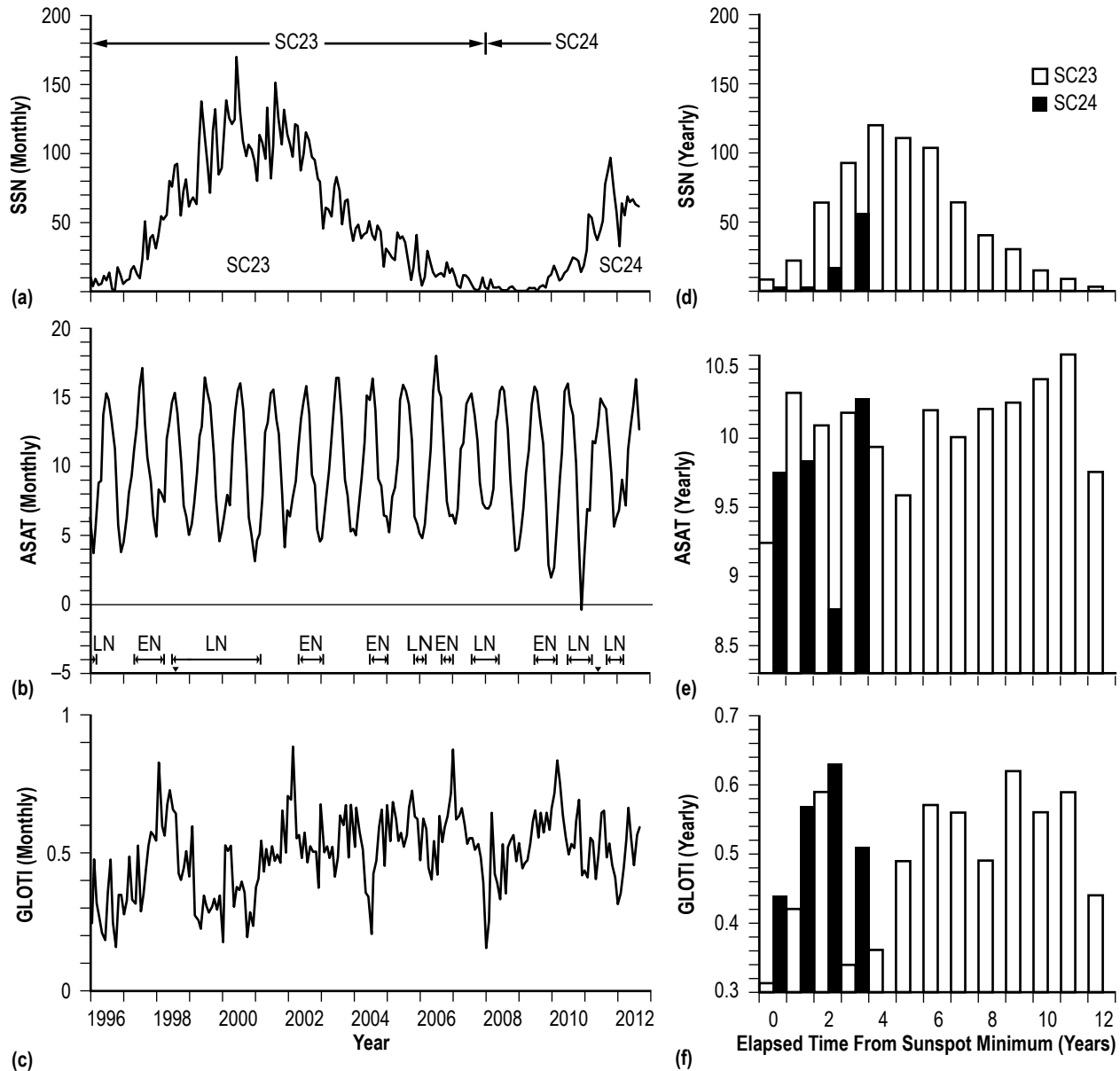


Figure 10. Variation of (a) SSN, (b) ASAT, and (c) GLOTI from January 1996–September 2012 and the variation of (d)  $\langle \text{SSN} \rangle$ , (e)  $\langle \text{ASAT} \rangle$ , and (f)  $\langle \text{GLOTI} \rangle$  for elapsed time in years past the sunspot minimum year for SC23 (the unfilled histograms) and SC24 (the filled histograms).

histograms). Based on yearly averages of SSN, SC23's sunspot minimum year was 1996, and SC24's sunspot minimum year was 2008. Also shown are the occurrences of EN (warm anomalies) and LN (cool anomalies) events as determined using monthly values of ONI, and the occurrence of significant volcanic eruptions (the small, filled triangles), those having a Volcanic Explosivity Index (VEI) of 4 or higher. (Occurrences of EN and LN events and significant volcanic eruptions have sometimes been associated with brief excursions in northern hemispheric and global temperatures.)<sup>104–107</sup>

It is interesting that EN events often appear to be associated with increases (warming) in the GLOTI (e.g., 2009), while LN events appear to be associated with decreases (cooling) in the GLOTI (e.g., 1998–2000). While conditions in the Niño 3.4 region presently remain slightly above average in temperature (ONI = 0.6 °C in October 2012; see <<http://cpc.ncep.noaa.gov>>), strictly speaking, they are reflective of the ENSO-neutral phase. Hence, while it appears unlikely that a fully-coupled EN will develop during the latter part of 2012 or in early 2013, the increased warming in the Niño 3.4 region is suggestive that the GLOTI will remain elevated for 2012 (see <<http://www.elno.noaa.gov>>, December 2012).

Also interesting is that every year of the first 4 years of SC24 has had higher GLOTI values than for the same elapsed time during SC23, although <SSN> and <ASAT> have generally been well below that occurring in SC23 for the same elapsed time from sunspot minimum. The first 4 years of SC24 have had an average GLOTI of about 0.54 °C, as compared to 0.24 °C for the first 4 years of SC23. So far this year (i.e., for January–September 2012), GLOTI is averaging 0.5 °C, as compared to the first nine months of 1990 of SC23 when it averaged only 0.37 °C. So, unless the October–December 2012 GLOTI values are extremely low (<−0.06 °C), elapsed time year four of SC24 also will have a GLOTI value higher than was seen in elapsed time year four of SC23 (=0.37 °C). Hence, presently it appears that SC24 will have <GLOTI> values higher than was seen for SC23 (=0.49 °C), unless, of course, the latter years of SC24 have cooler GLOTI values (<0.46 °C, assuming SC24 has PER = 12 years). (The year 2012 is now known to have ASAT = 9.7 °C and GLOTI = 0.56 °C. The ASAT value is lower in comparison to the same elapsed time for SC23, 9.93 °C; the GLOTI value is higher in comparison to the same elapsed time for SC23, 0.4 °C.)

Concerning the two significant volcanic eruptions occurring between 1996 and 2012, although both had VEI=4, neither eruption appears to have had any major, long-lasting effect on either ASAT or GLOTI. The two eruptions occurred on August 15, 1999 (Shiveluch, Kamchatka, Russia, 56.653° N., 161.36° E.) and June 4, 2011 (Puyehue, Chile, 40.59° S., 72.117° W.). The volcanic eruption data are available online at <<http://www.ngdc.noaa.gov>>.

### **2.3 Behavioral Aspects of ASAT and GLOTI During Rmin and Rmax Years**

Figure 11 displays the yearly averages of (a) Rmin (filled circles) and Rmax (filled triangles), (b) ASAT for Rmin years (filled circles) and GLOTI for Rmin years (filled triangles), and (c) ASAT for Rmax years (filled circles) and GLOTI for Rmax years (filled triangles) for SC9–SC24. Visually, the behaviors of the parameters are strikingly similar, especially the one between Rmax and Rmin.<sup>108,109</sup> While solar activity now appears to be tracking downwards, in contrast, ASAT and GLOTI are at or near record highs for SC23 and SC24.

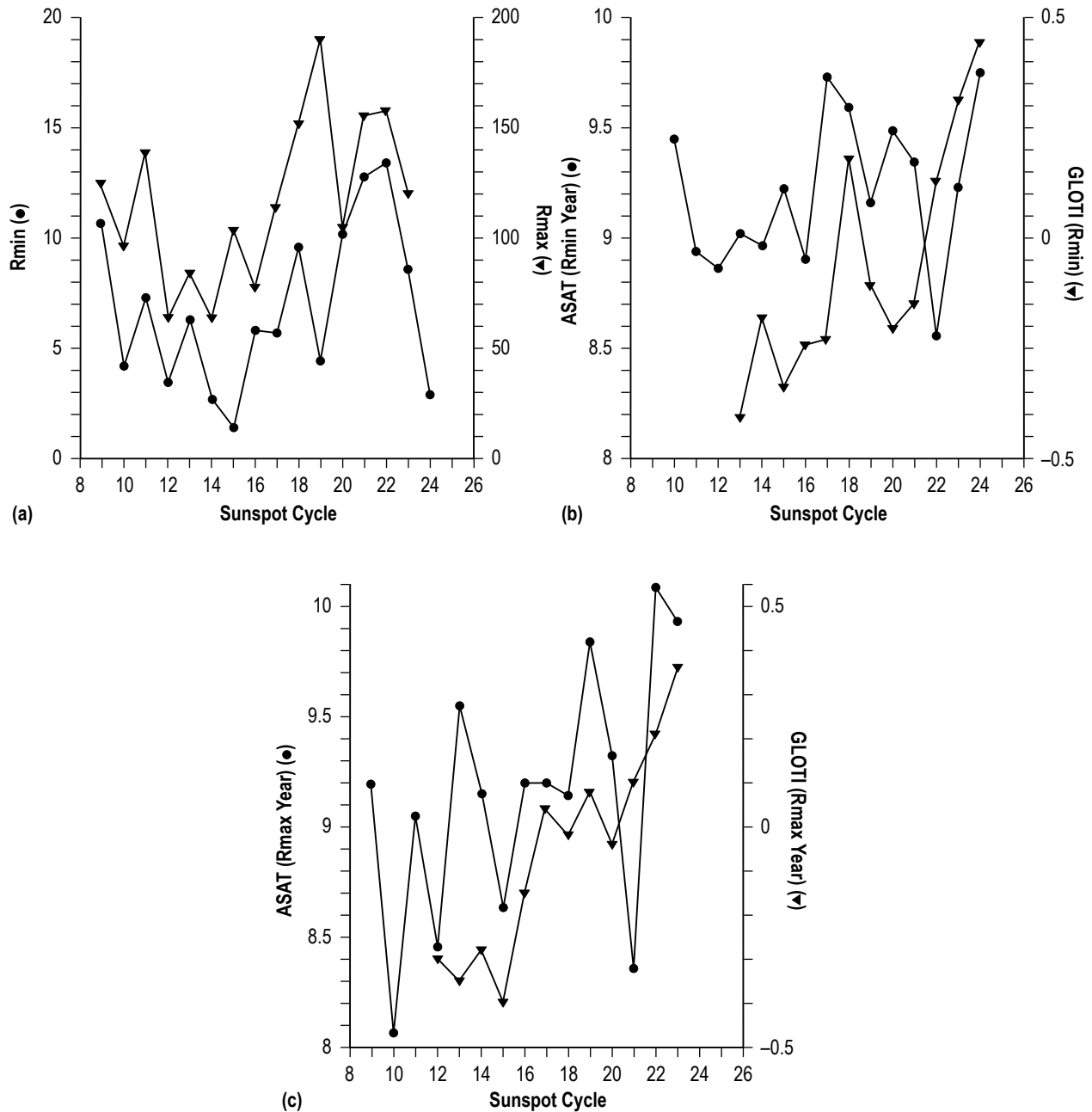


Figure 11. Yearly averages of (a) Rmin (filled circles) and Rmax (filled triangles), (b) ASAT for Rmin years (filled circles) and Rmax years (filled triangles), and (c) GLOTI for Rmin years (filled circles) and Rmax years (filled triangles) for SC9–SC24.

Figure 12 shows the scatter plots of (a) Rmax versus Rmin, (b) ASAT (Rmax year) versus ASAT (Rmin year), and (c) GLOTI (Rmax year) versus GLOTI (Rmin year), with the arrows located along the  $x$ -axes marking the values in the Rmin year for SC24. Concerning figure 12(a), it is apparent that one can easily predict the size of the ongoing cycle 2–4 years in advance from the Rmin value alone. Using SC9–SC23, one finds the inferred regression to be statistically important at  $cl > 95\%$ ,

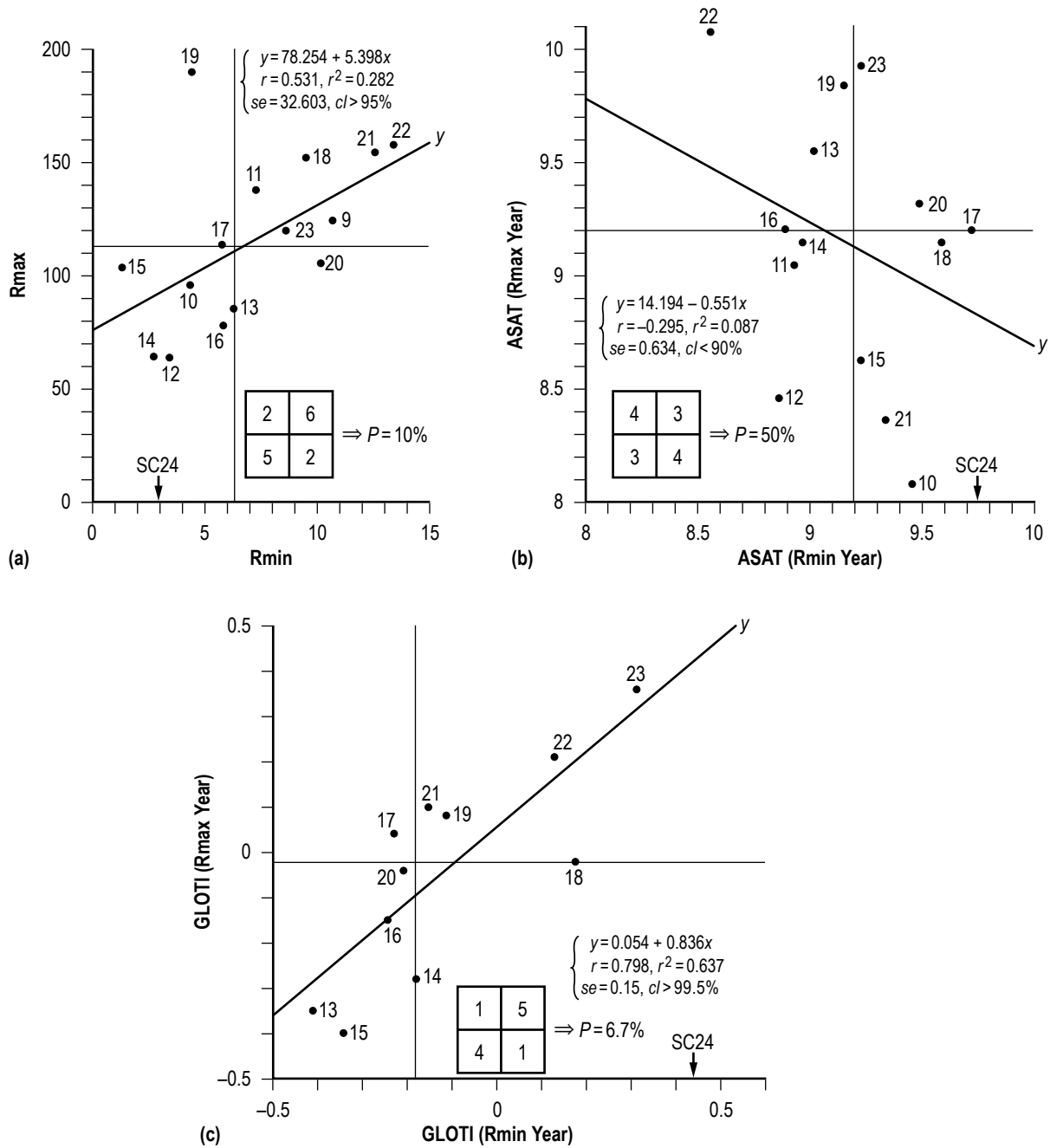


Figure 12. Scatter plots of (a) Rmax versus Rmin, (b) ASAT (Rmax year) versus ASAT (Rmin year), and (c) GLOTI (Rmax year) versus GLOTI (Rmin year), with the arrows located along the x-axes marking the values in the Rmin year for SC24.

having  $r=0.53$ . Applying the  $R_{\min}$  value for SC24 ( $=2.9$ ), one deduces the  $\pm 1$  *se* prediction interval for SC24's  $R_{\max}$  to be  $93.9 \pm 32.6$ , inferring that SC24 probably will have  $R_{\max} \geq 61.3$ , in close agreement to the predictions of de Jager and Duhau<sup>95</sup> and Wilson.<sup>97</sup> However, it is interesting that if one ignores SC19 (the largest  $R_{\max}$  SC), the resultant inferred regression becomes even stronger, having  $y=61.551+6.826x$ ,  $r=0.787$ ,  $r^2=0.619$ ,  $se=20.7$ , and  $cl>99.9\%$ , thus, yielding  $R_{\max}=81.3 \pm 20.7$  for SC24 (i.e.,  $R_{\max} \geq 60.6$ ). As previously noted, SSN for 2011 measures 55.7; hence, one anticipates 2012 to be the  $R_{\max}$  year for SC24 unless it proves to be a statistical outlier. (The January–September 2012 average of SSN is 59.5. The actual yearly value for SSN in 2012 turned out to be 57.5; the values in 2013 for January–May average about 62.)

The inferred fit for ASAT ( $R_{\max}$  year) versus ASAT ( $R_{\min}$  year), having  $r=-0.295$ , is not statistically important ( $cl<90\%$ ); however, the inferred fit for GLOTI ( $R_{\max}$  year) versus GLOTI ( $R_{\min}$  year) is statistically important, having  $r=0.798$ ,  $se=0.15$  °C and  $cl>99.5\%$ . Applying the GLOTI ( $R_{\min}$  year) $=0.44$  °C, one estimates that GLOTI ( $R_{\max}$  year) $=0.42 \pm 0.15$  °C, or GLOTI ( $R_{\max}$  year)  $<0.57$  °C, for SC24. For comparison, SC23 had GLOTI ( $R_{\max}$  year) $=0.36$  °C. Interestingly, both ASAT and GLOTI values for the  $R_{\min}$  year are the warmest values on record for an  $R_{\min}$  year, being 9.75 °C and 0.44 °C, respectively. Perhaps this is a strong indication that both ASAT and GLOTI in the  $R_{\max}$  year for SC24 will exceed respective record values, being 10.07 °C in SC22 for ASAT and 0.36 °C in SC23 for GLOTI.

Figure 13 shows the cyclic secular trend over SC9–SC23 for (a) ASAT ( $R_{\min}$  year), (b) GLOTI ( $R_{\min}$  year), (c) ASAT ( $R_{\max}$  year), and (d) GLOTI ( $R_{\max}$  year). While the inferred regressions for ASAT are not statistically important, those based on Fisher's exact test do suggest a real secular rise in ASAT ( $R_{\min}$  year) and ASAT ( $R_{\max}$  year) over time. Hence, values of ASAT ( $R_{\min}$  year) and ASAT ( $R_{\max}$  year) appear to be slowly rising with the passage of time such that SC24 and later cycles more often than not should have ASAT ( $R_{\min}$  year) and ASAT ( $R_{\max}$  year) values warmer than their median values. In fact, since SC17, six of eight SCs have had ASAT ( $R_{\min}$  year) values warmer than 9.23 °C, and since SC16, seven of eight cycles have had ASAT ( $R_{\max}$  year) values warmer than 9.2 °C. Based on the inferred regressions, one expects ASAT ( $R_{\max}$  year) $=9.67 \pm 0.59$  °C (or ASAT ( $R_{\max}$  year)  $<10.26$  °C) for SC24 and ASAT ( $R_{\min}$  year) $=9.37 \pm 0.45$  °C (or ASAT ( $R_{\min}$  year)  $<9.82$  °C) for SC25.

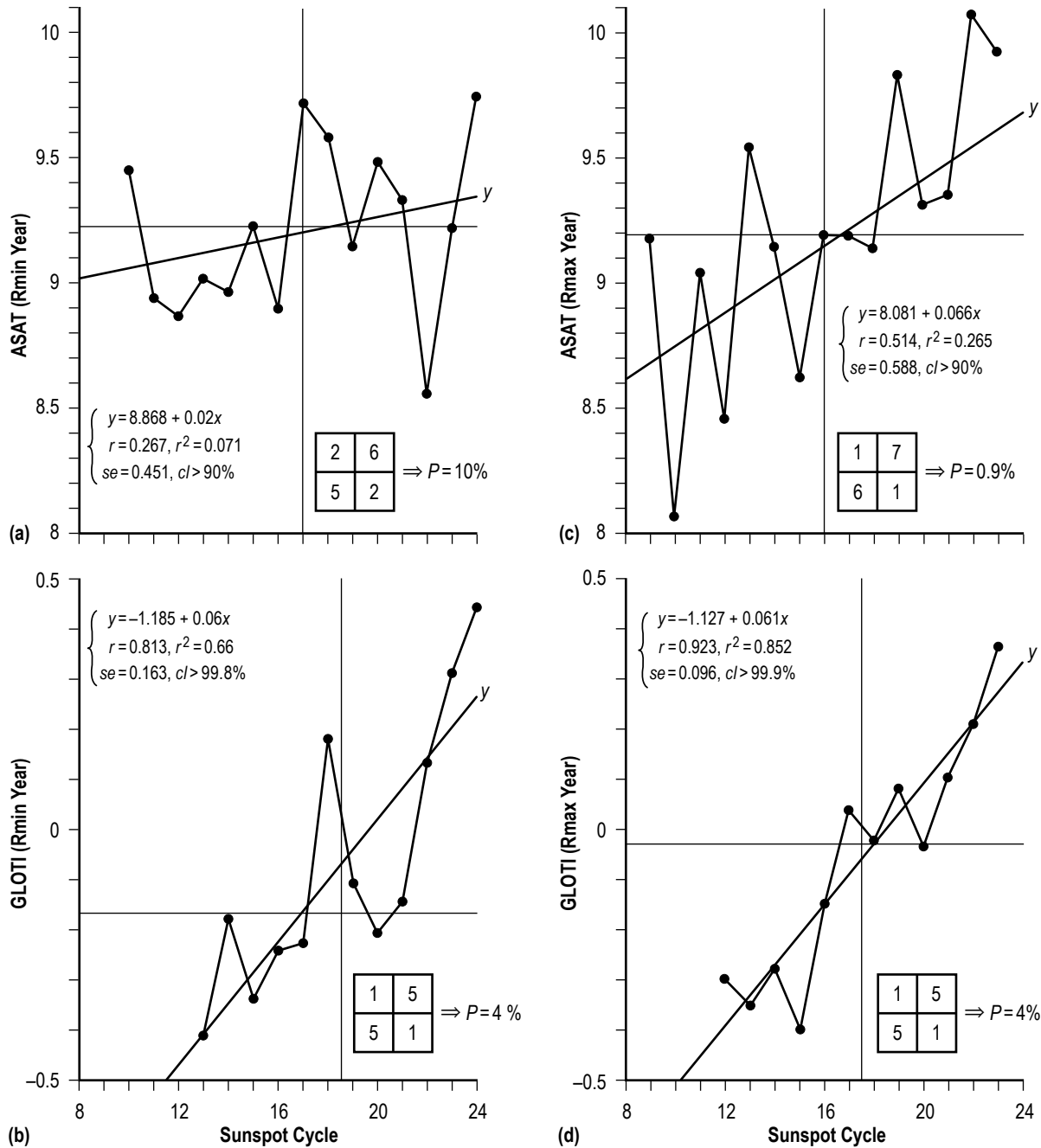


Figure 13. Cyclic secular trend over SC9–SC23 of (a) ASAT (Rmin year), (b) GLOTI (Rmin year), (c) ASAT (Rmax year), and (d) GLOTI (Rmax year).

For GLOTI, both the inferred regressions and Fisher's exact tests reveal GLOTI (Rmin year) and GLOTI (Rmax year) to be statistically important, suggesting warmer values with the passage of time. For SC24, one estimates GLOTI (Rmax year) =  $0.34 \pm 0.1$  °C, (or GLOTI (Rmax year)  $< 0.44$  °C) and for SC25, one estimates GLOTI (Rmin year) =  $0.32 \pm 0.16$  °C (or GLOTI (Rmin year)  $< 0.48$  °C).



Figure 14 shows the scatter plots of (a) ASAT (Rmin year) and (b) GLOTI (Rmin year) versus Rmin. Neither parameter is found to display a statistically meaningful association. So, while the cyclic secular trends (see fig. 13) provide some indication as to the values of ASAT (Rmin year) and GLOTI (Rmin year), the actual value of the Rmin itself provides no clear indication as to the expected values of ASAT or GLOTI for the Rmin year.

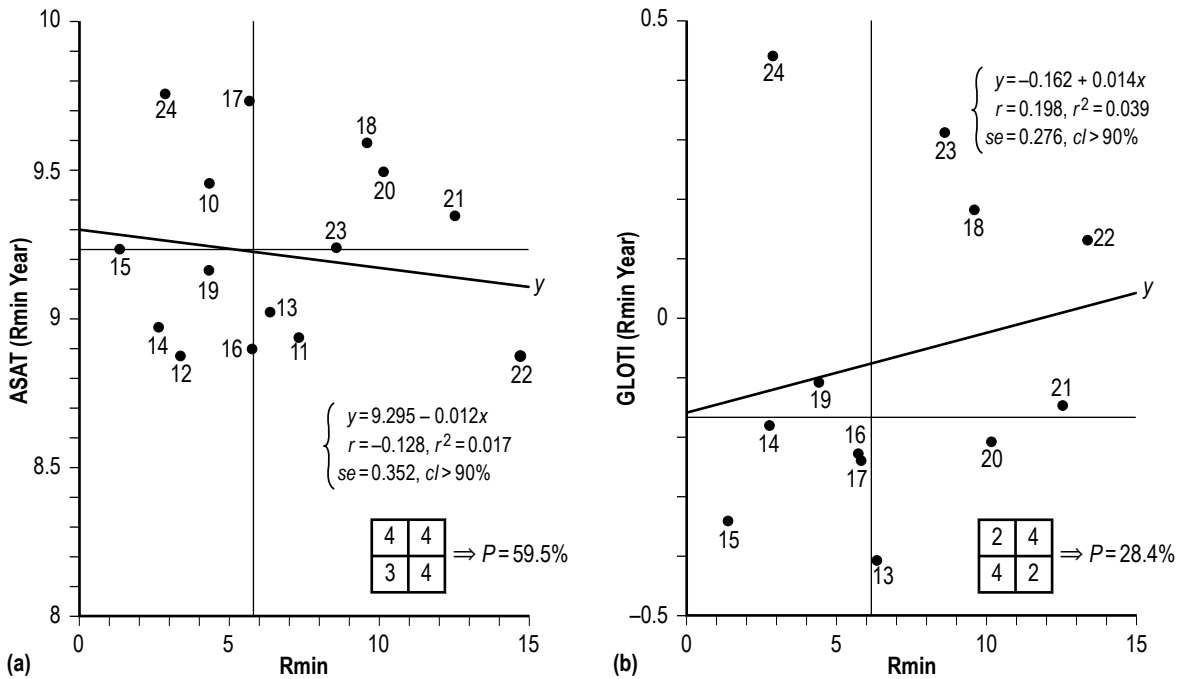


Figure 14. Scatter plots of (a) ASAT (Rmin year) and (b) GLOTI (Rmin year) versus Rmin.

Figure 15 depicts the scatter plots of (a) ASAT (Rmax year) and (b) GLOTI (Rmax year) versus Rmax. While the inferred linear correlation between ASAT (Rmax year) and Rmax is only of marginal statistical importance ( $r = 0.36$ ,  $cl > 90\%$ ), the inferred linear regression between GLOTI (Rmax year) and Rmax is highly statistically important ( $r = 0.67$ ,  $cl > 98\%$ ). Presuming  $R_{max} = 70$  for SC24, one infers  $ASAT (R_{max} \text{ year}) = 8.93 \pm 0.46 \text{ } ^\circ\text{C}$ , or  $ASAT (R_{max} \text{ year}) < 9.39 \text{ } ^\circ\text{C}$ , and  $GLOTI (R_{max} \text{ year}) = -0.23 \pm 0.19 \text{ } ^\circ\text{C}$ , or  $GLOTI (R_{max}) < -0.04 \text{ } ^\circ\text{C}$ . It is noteworthy that all previous cycles having  $R_{max} < 110.2$  (the median  $R_{max}$  based on SC12–SC23) have had  $GLOTI (R_{max} \text{ year}) < -0.03 \text{ } ^\circ\text{C}$ . Hence, one strongly expects  $GLOTI (R_{max} \text{ year})$  to be  $< -0.04 \text{ } ^\circ\text{C}$  based on the expected  $R_{max} = 70$  (or smaller) for SC24, unless, of course, SC24 proves to be a statistical outlier, which now seems highly likely (based on GLOTI values for 2012 and expected values for 2013).

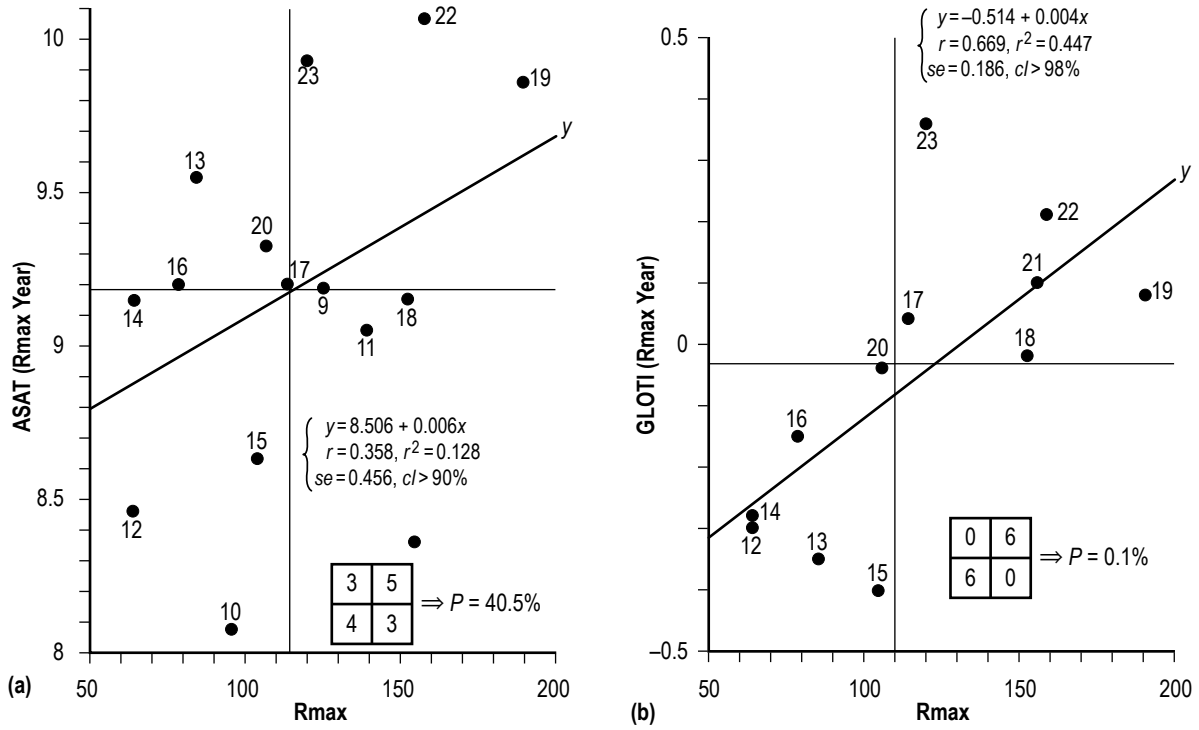


Figure 15. Scatter plots of (a) ASAT (Rmax year) and (b) GLOTI (Rmax year) versus Rmax.

Regarding the inferred correlation between GLOTI (Rmax year) and Rmax, even though the fit is considered to be highly statistically important,<sup>110</sup> it is noteworthy that, relative to its regression value ( $-0.04\text{ }^{\circ}\text{C}$  based on  $R_{\text{max}} = 119.6$ ), SC23's GLOTI (Rmax year) is about  $2.1\text{ } se$  warmer ( $=0.36\text{ }^{\circ}\text{C}$ , the warmest observed value in the modern era); therefore, if SC24's GLOTI (Rmax year) behavior proves similar to that of SC23's, then one cannot discount the possibility that GLOTI (Rmax year) for SC24 will be a positive value, perhaps considerably warmer than its inferred value of  $GLOTI(R_{\text{max}}\text{ year}) = -0.23 \pm 0.19\text{ }^{\circ}\text{C}$ , using  $R_{\text{max}} = 70$ .

#### 2.4 Behavioral Aspects of ASAT and GLOTI Relative to the AMO Index and the Trend in the Atmospheric Concentration of Carbon Dioxide at Mauna Loa, Hawaii

As noted in section 2.3, factors other than solar forcing now appear to be the stronger factors influencing the Earth's climate system, at least over the past few decades. Examined here are the relations between the ASAT and GLOTI values against the AMO index values and the trend in the atmospheric concentration of carbon dioxide ( $\text{CO}_2$ ) values as measured at Mauna Loa, Hawaii, for the interval 1950–2011, an interval that includes the current period when solar forcing of climate appears to have weakened.

The AMO is a temperature oscillation in the detrended sea surface temperature of the North Atlantic Ocean (0–70° N.) having a period of about 65–70 years that fluctuates between warm (positive) and cool (negative) phases.<sup>111,112</sup> It is presently in its warm phase, having begun about 1995 based on 10-yma values, with the minimum 10-yma value of the AMO index prior to the present warming phase occurring about 1975 (i.e., although the warm phase began about 1995, the trend in the warming began about 1975). The warmest 10-yma value of the AMO index for the current warm phase presently measures about 0.21 °C and is about 0.06 °C warmer than the preceding peak 10-yma value that was seen in the last warming period (about 1956). It is warmer by about 0.11 °C than the peak 10-yma value that was seen about 1876. The current warming phase is expected to last at least another one to two decades. Values of the monthly AMO index are available online at <<http://www.esrl.noaa.gov/psd/data/correlation/amon.us.long.data>>.

Carbon dioxide is the major constituent of the greenhouse gases in the Earth's atmosphere,<sup>113–116</sup> although other anthropogenic gases contribute as well, such as methane and nitrous oxide, but to a lesser extent as compared to CO<sub>2</sub>.<sup>117</sup> Continuous measurement of the atmospheric concentration of CO<sub>2</sub> has been ongoing at Mauna Loa since 1958.<sup>118–120</sup> While the atmospheric concentration of CO<sub>2</sub> is found to vary seasonally over the year, expressed as an annual average, it has been increasing unabatedly year-to-year from a mean of 315.97 ppm in 1959 to 391.57 ppm in 2011, yielding an average rate of increase of about 1.45 ppm per year or about 14.54 ppm per decade. Annual averages of the Mauna Loa CO<sub>2</sub> (MLCO<sub>2</sub>) measurements, expressed in ppm, are available online for the interval 1959–2011 at <[ftp://ftp.cmdl.noaa.gov/ccg/co2/trends/co2\\_annmean\\_mlo.txt](ftp://ftp.cmdl.noaa.gov/ccg/co2/trends/co2_annmean_mlo.txt)> and annual values of the global radiative forcing due to greenhouse gases are available online for the interval 1979–2011 at <<http://www.esrl.noaa.gov/gmd/aggi/>>. (MLCO<sub>2</sub> measured 393.82 ppm in 2012.)

Figure 16 shows the annual (thin jagged line) and 10-yma (thick smoothed line) of (a) the AMO index and (b) the MLCO<sub>2</sub> values for the interval 1950–2011. Regarding the variation of figure 16(a), it was reflective of the cool phase (negative 10-yma values) during the interval 1965–1994 and the warm phase (positive 10-yma values) both prior to 1965 and after 1994. As noted previously, the present warming, as deduced using the 10-yma values, measured at least 0.21 °C in 2002 and 2006, up from the cooling, which measured –0.25 °C in 1974 and 1975. The previous warming peaked at 0.15 °C in 1956. (The current warming is expected to continue for at least another 20 years, possibly exceeding 0.21 °C.)

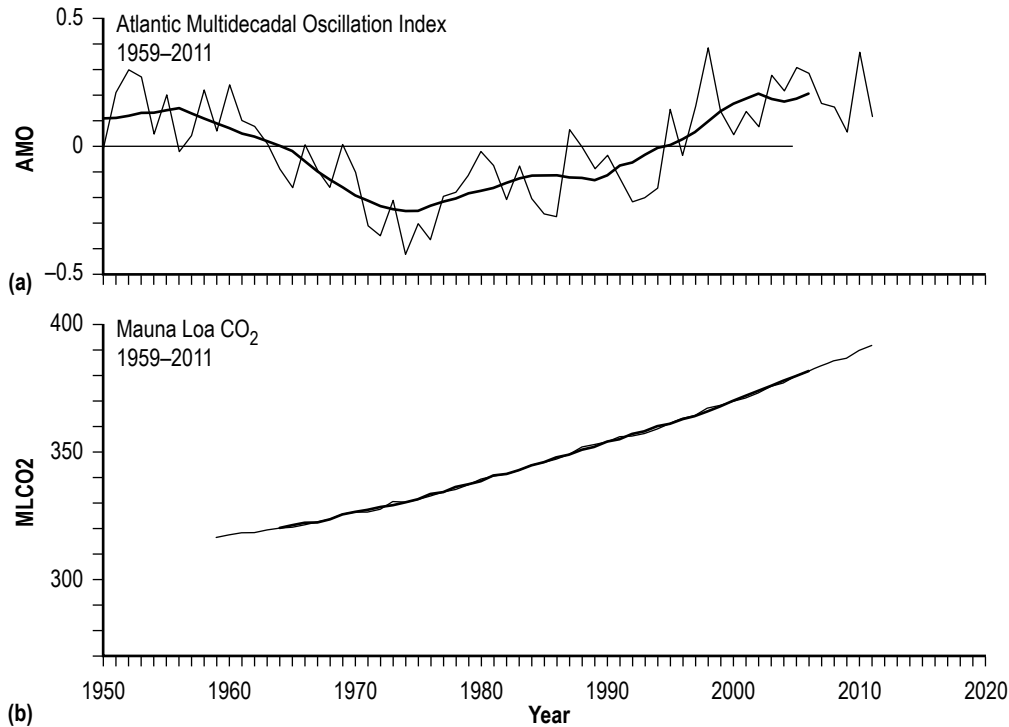


Figure 16. Annual (thin jagged line) and 10-yma (thick smoothed line) of (a) the AMO index and (b) the MLCO2 values for the interval 1950–2011.

Regarding figure 16(b), visually, the annual and 10-yma values are virtually identical. The 10-yma value of MLCO2 measures about 320 ppm in 1964 and about 382 ppm in 2006, an increase of about 19% in 42 years. Hence, based on the trend, atmospheric concentration of CO<sub>2</sub> at Mauna Loa is growing at an average rate of about 1.48 ppm per year, or 14.8 ppm per decade, with no evidence suggesting a leveling off. In fact, placement of a straight-edge along the curve shows that the MLCO2 values actually are increasing faster than at a linear rate, which should be of great concern, especially because of the predicted consequences directly attributable to increased anthropogenic gases in the Earth's atmosphere (and the associated warming of the atmosphere and oceans).<sup>121–128</sup>

Figure 17 displays the scatter plots of (a) ASAT and (b) GLOTI against the AMO index for the interval 1950–2006 based on 10-yma values. Two fits are shown in each subpanel with selected years identified (1950, 1975, 1976, and 2006). The lower fit is based on the interval 1950–1975, where the year 1975 represents the coolest extreme in the AMO index, and the upper fit is based on the interval 1976–2006, which is the current interval of continuous warming from its coolest AMO index value in 1975. Concerning figure 17(a), both fits are found to be statistically important, with the lower fit having  $r=0.85$  and  $cl>99.9\%$  and the upper fit having  $r=0.97$  and  $cl\gg99.9\%$ . Concerning figure 17(b), only the upper fit is found to be statistically important, having  $r=0.99$  and  $cl\gg99.9\%$ . Apparently, the ASAT and GLOTI values are now more strongly coupled to the AMO than they were prior to 1976. (The 10-yma values for the year 2007 for ASAT and GLOTI are 10.01 °C and 0.59 °C, respectively. The 10-yma value of AMO for 2007 is 0.206 °C.)

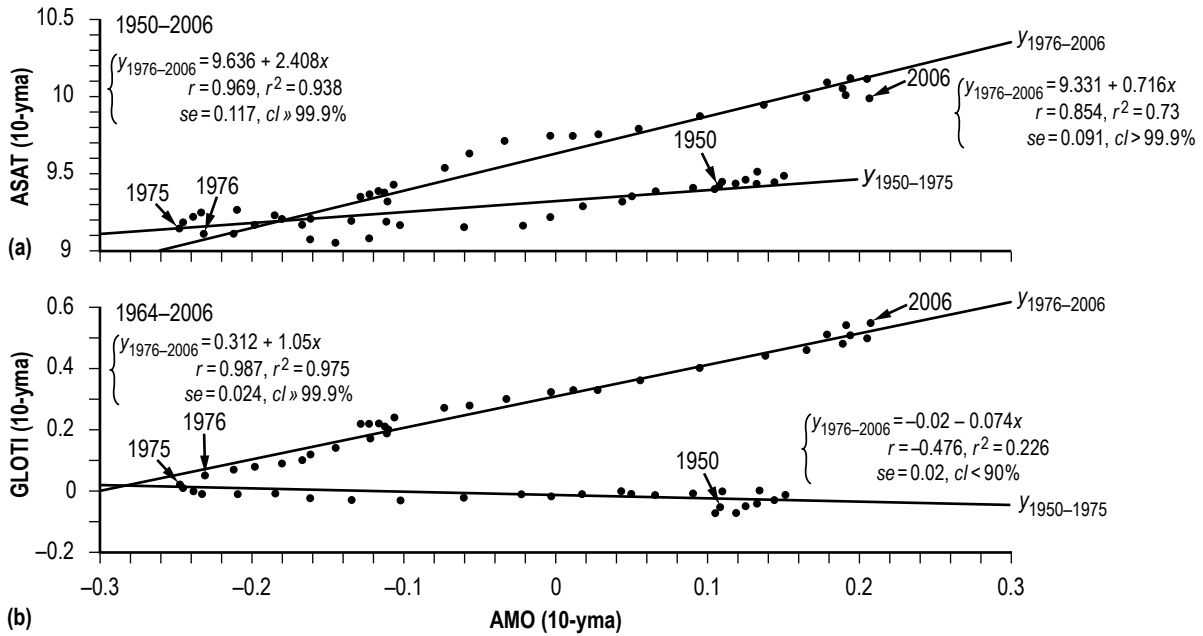


Figure 17. Scatter plots of (a) ASAT and (b) GLOTI against the AMO index for the interval 1950–2006, based on 10-yma values.

Figure 18 shows the scatter plots of (a) ASAT and (b) GLOTI versus the MLCO2 values for the interval 1964–2006 based on 10-yma values. Concerning figure 18(a), using all available values (denoted  $y_{1964-2006}$ ), the fit, while appearing to be statistically important, is found not to be statistically important ( $r=0.91$ ,  $cl<90\%$ ). However, when the comparison is based on the shortened interval 1982–2003 (denoted  $y_{1982-2003}$ ), the association between ASAT and MLCO2 is indeed found to be statistically important ( $r=0.99$ ,  $cl>99.9\%$ ). Concerning figure 18(b), it is inferred to be highly statistically important ( $r=0.99$ ,  $cl>>99.9\%$ ). (The 10-yma of MLCO2 for 2012 is 383.67 ppm.)

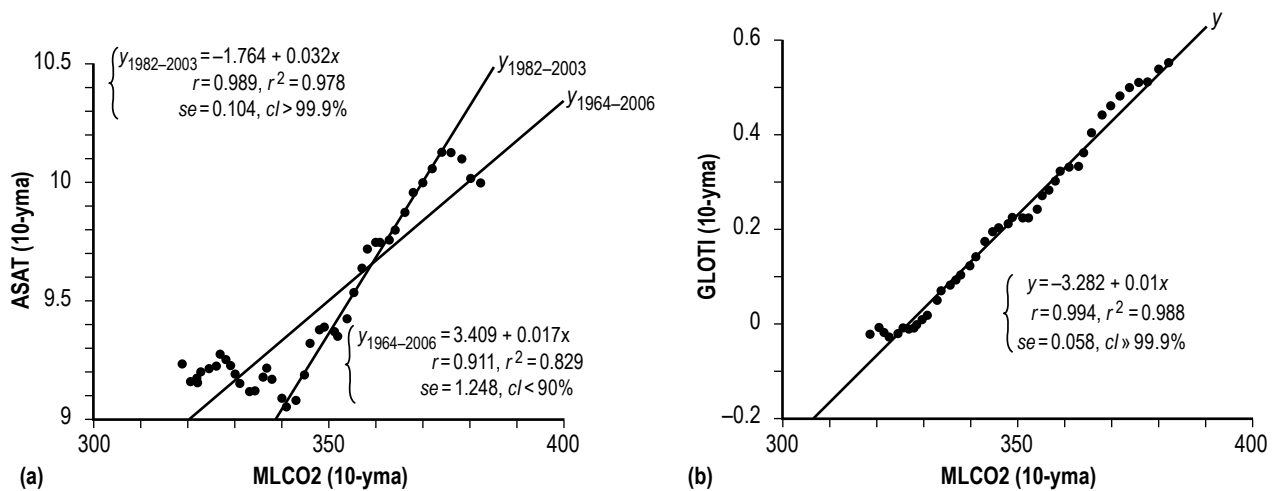


Figure 18. Scatter plots of (a) ASAT and (b) GLOTI versus the MLCO2 values for the interval 1964–2006, based on 10-yma values.

### 3. DISCUSSION AND CONCLUSIONS

This TP has shown (see fig. 1) that the annual temperature as measured at the Armagh Observatory and the temperature anomaly as described by the GLOTI have both revealed a warming planet Earth over the past century or more, with temperatures increasing at the average rate of  $0.14\text{ }^{\circ}\text{C}$  per decade based on the ASAT and  $0.09\text{ }^{\circ}\text{C}$  per decade based on the GLOTI.<sup>81,82,129,130</sup> Although the two parameters both show general long term secular increases over time, their individual behaviors sometimes have differed. For example, the rise in temperature between about 1980 and 2007 at Armagh appears to have been much steeper than was seen for the GLOTI. Likewise, while temperature was trending downwards between about 1945 and 1980 at Armagh, it is perceived to have been relatively flat as measured by the GLOTI during the same interval. Additionally, because the ASAT record begins in 1844 and the GLOTI record does not begin until 1880, the ASAT values have an advantage over the GLOTI values for determining temperatures prior to 1880. During this earlier epoch, the temperature at Armagh actually is found to have been warmer than its long term mean  $+1\text{ }sd$  of  $9.25 \pm 0.55\text{ }^{\circ}\text{C}$  and clearly was trending downwards from about 1845 to 1880. While true, the yearly values of the ASAT now being experienced are among the warmest ever recorded at Armagh, with the trend line now being warmer than was seen previously in 1849 by more than  $0.5\text{ }^{\circ}\text{C}$ , surpassing the 10-yma values of 1849 about the year 1990.

Also shown in this investigation is that, while the behavior of SSN, ASAT, and GLOTI are strikingly similar, especially prior to SC21, the trends in temperature and SSN now no longer appear to be closely coupled. Hence, one surmises that other factors must now be dominating the Earth's climate system, at least over the past three SCs (i.e., since SC21).<sup>131,132</sup> The trend in the GLOTI values remains upwards in 2006 (the last available 10-yma value), while the trend in the SSN values quite noticeably is downwards. The trend in the ASAT values appears to have peaked locally in 2002/2003, cooling slightly by  $0.13\text{ }^{\circ}\text{C}$  between 2003 and 2006. While true, it is anticipated that the trend in the ASAT values soon will flatten and then again continue to rise thereafter, especially given that the AMO remains in the warm phase and  $\text{CO}_2$  continues to build up in the Earth's atmosphere.

Clearly, the ASAT and GLOTI values track each other very well, with 70% of the yearly values obeying the paradigm of warmer (cooler) temperatures at Armagh being indicative of a warmer (cooler) temperature anomaly as measured by the GLOTI. However, a strange behavior (see fig. 4) has been found involving the 10-yma values of the two parameters. Namely, two separate regressions are inferred to link the GLOTI and ASAT values. The first regression spans 1885–1945, having  $r=0.85$ ,  $r^2=0.72$ , and  $se=0.06\text{ }^{\circ}\text{C}$ . The second regression spans the current interval 1982–2006, having  $r=0.96$ ,  $r^2=0.93$ , and  $se=0.04\text{ }^{\circ}\text{C}$ . The interval between 1945 and 1982 appears to be one of transition with 10-yma values of ASAT displaying cooling and 10-yma values of GLOTI displaying a near flat appearance. The two regressions are offset by about  $0.3\text{ }^{\circ}\text{C}$ , with the current values being warmer. Hence, while a 10-yma value of ASAT equal to  $9.5\text{ }^{\circ}\text{C}$  as measured in 1942 yields a 10-yma GLOTI of about  $-0.05\text{ }^{\circ}\text{C}$ , such a value now yields a 10-yma value of GLOTI equal to about  $0.27\text{ }^{\circ}\text{C}$ , a difference of  $0.32\text{ }^{\circ}\text{C}$ . It is unclear as to what may have caused the relationship between the 10-yma values of GLOTI and ASAT to change and be displaced upwards by about  $0.32\text{ }^{\circ}\text{C}$ .

This TP also has shown that the cyclic variation of the  $\langle \text{ASAT} \rangle$  and  $\langle \text{GLOTI} \rangle$  has been decidedly upwards towards warmer temperatures since SC12, with no evidence of flattening or cooling except for a brief interval between SC18 and SC21 (see fig. 7). While cyclic averages of  $\langle \text{SSN} \rangle$  clearly are now tracking downwards (since SC21), cyclic averages of  $\langle \text{ASAT} \rangle$  and  $\langle \text{GLOTI} \rangle$  remain tracking upwards towards warmer temperatures. Hence, solar forcing of Earth's climate system, which should result in cooling if it remained the main forcing factor in climatic change, now seems to have been overwhelmed by other factors, factors that have resulted in a continued warming as shown by the ASAT and GLOTI values, even as solar activity has declined. Clearly, SC23 was warmer than SC22, which was warmer than SC21. The inference then is that the temperature at Armagh possibly could be warmer in SC24 as compared to what it was in SC23 and that the  $\langle \text{GLOTI} \rangle$  values possibly could be higher as well.

Figure 19 replots figures 7(e) and (f) as linear fits of (a)  $\langle \text{ASAT} \rangle$  and (b)  $\langle \text{GLOTI} \rangle$  versus SC for SC12–SC23. Both fits are inferred to be highly statistically important. Using the preferred fits ( $y$ ) based on SC12–SC23, one estimates SC24 to likely have  $\langle \text{ASAT} \rangle = 9.82 \pm 0.24 \text{ }^\circ\text{C}$  and  $\langle \text{GLOTI} \rangle = 0.37 \pm 0.09 \text{ }^\circ\text{C}$  (the  $\pm 1 \text{ se}$  prediction intervals), inferring only about a 16% chance that  $\langle \text{ASAT} \rangle$  and  $\langle \text{GLOTI} \rangle$  for SC24 will be  $>10.06 \text{ }^\circ\text{C}$  and  $>0.46 \text{ }^\circ\text{C}$ , respectively. Hence, one easily could conclude that it appears unlikely that SC24 will have  $\langle \text{ASAT} \rangle$  and  $\langle \text{GLOTI} \rangle$  values warmer than was seen in SC23 (i.e.,  $10.08 \text{ }^\circ\text{C}$  and  $0.49 \text{ }^\circ\text{C}$ , respectively), as suggested by Solheim et al.<sup>61</sup> (In figure 19, the error bars represent the mean  $\pm 1 \text{ sd}$  interval for each cycle.)

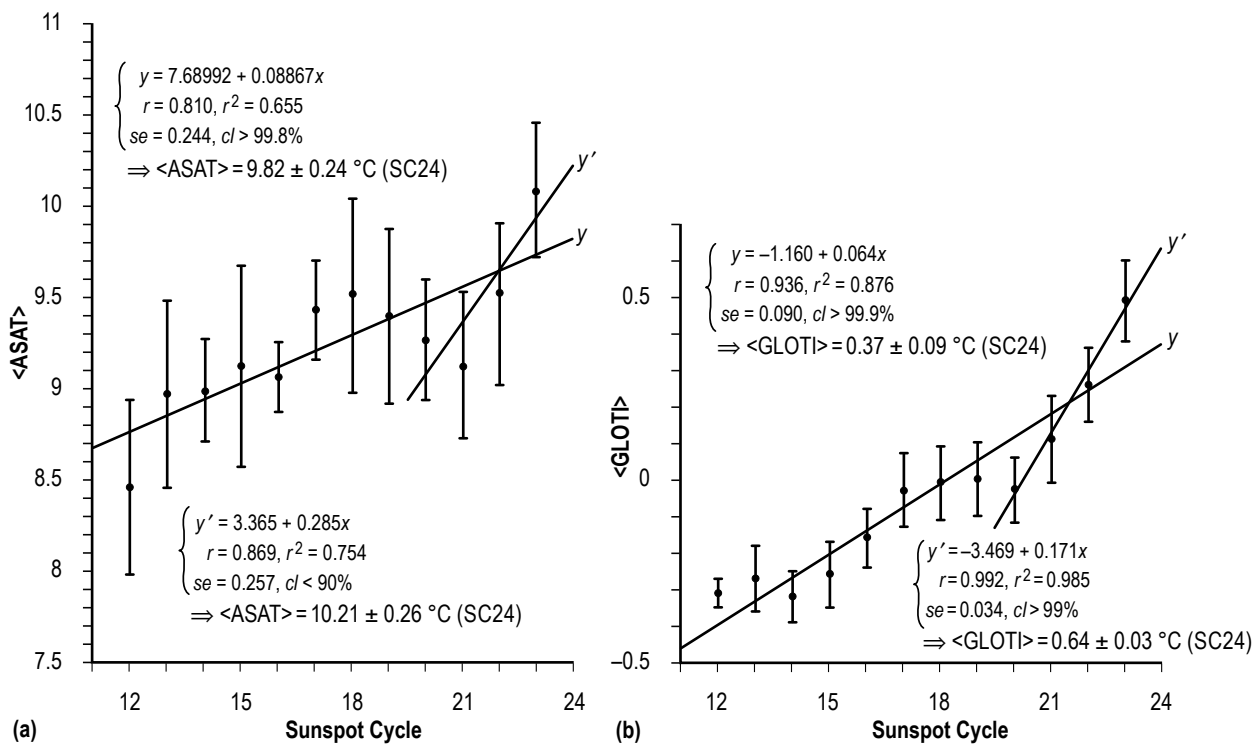


Figure 19. Linear fits of (a)  $\langle \text{ASAT} \rangle$  and (b)  $\langle \text{GLOTI} \rangle$  versus SC for SC12–SC23.



However, alternate regressions ( $y'$ ) plotted in figure 19 based only on the most recent SCs (SC20–SC23) counter this conclusion, where these more recent cycles suggest a faster warming from one cycle to the next than was seen in the earlier cycles. While the inferred regression for <ASAT> does not appear to be statistically important, the one for <GLOTI>, in contrast, is found to be highly statistically important ( $r=0.99$ ,  $cl>99\%$ ). Hence, presuming the validity of the alternate regression fit, <GLOTI> is inferred to be about  $0.64 \pm 0.03$  °C for SC24, thus suggesting that SC24 undoubtedly will be warmer than SC23, with only about a 16% chance of being cooler than  $0.61$  °C, a value at least  $0.12$  °C warmer than was seen in SC23 ( $0.49$  °C).

It should be noted that in this analysis, SC23 (1996–2007) stands out as having <ASAT> and <GLOTI> values considerably warmer (the warmest of any modern era SC on record) than would have been expected based on its observed Rmax or <SSN> (see fig. 8). Likewise, most unusual are the values of the ASAT and GLOTI for the year 2010, a year when the ASAT had the lowest temperature ( $8.75$  °C) since 1986, yet the GLOTI had the highest temperature anomaly ( $0.63$  °C).

For SC24's Rmax year (believed to be either the year 2012 or 2013), the inferred regression of GLOTI (Rmax year) versus SC suggests a value of about  $0.34 \pm 0.1$  °C (the  $\pm 1$  *se* prediction interval) for GLOTI (see fig. 13). Based on its expected Rmax value of about 70, GLOTI (Rmax year) is expected to be only about  $-0.23 \pm 0.19$  °C (see fig. 15). Presently, the GLOTI values for 2012 are averaging about  $0.5$  °C (based on the January–September average). Hence, if the year 2012 proves to be the Rmax year, it will be the warmest such year on record, exceeding that measured for SC23 ( $0.46$  °C in the year 2000). (For GLOTI, the year 2012 measured  $0.56$  °C.)

Comparisons of 10-yma values of the ASAT and GLOTI against the AMO index show that the current interval 1976–2006 (SC21–present) has inferred regressions that are highly statistically important ( $r=0.97$  and  $cl \gg 99.9\%$  for ASAT and  $r=0.99$  and  $cl \gg 99.9\%$  for GLOTI), suggesting that the current interval is one where the ASAT and GLOTI values are highly coupled with the AMO. Ten-yma values of the AMO index values exceeding  $0.2$  °C are suggestive that 10-yma values of ASAT  $\geq 10$  °C and GLOTI values  $\geq 0.5$  °C. (The AMO index currently reflects a continuing warming phase, one that is expected to persist for at least 10–20 years or more. Furthermore, the 10-yma value of AMO exceeded  $0.2$  °C in 2006 and 2007.)

Comparisons of 10-yma values of the ASAT and GLOTI against the 10-yma values in MLCO2 for the interval 1964–2006 show that, while the inferred regression of ASAT versus MLCO2 does not appear to be statistically important, the one for the GLOTI versus MLCO2 is inferred to be highly statistically important ( $r=0.99$  and  $cl \gg 99.9\%$ ). Because the trend in MLCO2 values clearly is upwards, increasing at the average rate of about  $1.48$  ppm per year based on the 10-yma values, atmospheric concentration of CO<sub>2</sub> at Mauna Loa probably will exceed 400 ppm by the year 2015. A 10-yma value of MLCO2 equal to 400 ppm suggests a 10-yma value of GLOTI equal to about  $0.72 \pm 0.06$  °C (see fig. 18).

In conclusion, the trend in temperature at Armagh now appears to be strongly coupled with the trend in the AMO. Likewise, the GLOTI now appears to be strongly coupled to both the trends in the AMO and the level of atmospheric concentration of CO<sub>2</sub> as measured at Mauna Loa. Since the trend in AMO remains reflective of the warm phase, which is expected to persist for the next decade



or longer, the trend in yearly temperatures at Armagh is expected to continue to be warmer than the long term average ( $9.25 \pm 0.55$  °C) and may even rise to new record highs (i.e., annually  $>10.6$  °C, 10-yr trend value  $>10.13$  °C). Similarly, the trend in the GLOTI values is expected to continue to rise, especially because of the continuing rise in the trend of the anthropogenic gases in the Earth's atmosphere. As to whether the <ASAT> and <GLOTI> values will be warmer in SC24 as compared to that seen in SC23 (i.e.,  $10.08$  °C for <ASAT> and  $0.49$  °C for <GLOTI>), presently, one cannot be completely certain. Based on the first 4 years of SC24 (2008–2011), the ASAT is averaging  $9.65 \pm 0.65$  °C in SC24, as compared to  $9.96 \pm 0.5$  °C in the first 4 years of SC23 (1996–1999), while the GLOTI is averaging  $0.54 \pm 0.08$  °C in the first 4 years of SC24, as compared to  $0.42 \pm 0.13$  °C in the first 4 years of SC23.



## REFERENCES

1. Gray, L.J.; Beer, J.; Geller, M.; et al.: “Solar Influences on Climate,” *Rev. Geophys.*, Vol. 48, No. 4, 53 pp., doi:10.1029/2009RG000282, December 2010.
2. Herschel, W.: “Observations tending to investigate the Nature of the Sun, in order to find the Causes or Symptoms of its variable Emission of Light and Heat; with Remarks on the Use that may possibly be drawn from Solar Observations,” *Philos. T. R. Soc. Lon.*, Vol. 91, pp. 265–318, doi:10.1098/rstl.1801.0015, April 16, 1801.
3. Beer, J.; Mende, W.; and Stellmacher, R.: “The role of the sun in climate forcing,” *Quaternary Sci. Rev.*, Vol. 19, Nos. 1–5, pp. 403–415, January 2000.
4. Rind, D.: “The Sun’s Role in Climate Variations,” *Science*, Vol. 296, pp. 673–677, doi:10.1126/science.1069562, April 26, 2002.
5. Haigh, J.D.: “The Effects of Solar Variability on the Earth’s Climate,” *Philos. T. R. Soc. Lon. A*, Vol. 361, No. 1802, pp. 95–111, January 15, 2003.
6. de Jager, C.: “Solar Forcing of Climate. 1: Solar Variability,” *Space Sci. Rev.*, Vol. 120, Nos. 3–4, pp. 197–241, doi:10.1007/s11214-005-7046-5, 2005.
7. de Jager, C.: “Solar forcing of climate,” *Surv. Geophys.*, Vol. 33, Nos. 3–4, pp. 445–451, doi:10.1007/s10712-012-9193-z, 2012.
8. Schwabe, M.: “Sonnenbeobachtungen im Jahre 1843,” *Astron. Nachr.*, Vol. 21, p. 233, 1844.
9. Izenman, A.J.; “J.R. Wolf and H.A. Wolfer: An Historical Note on the Zürich Sunspot Relative Numbers,” *J. R. Stat. Soc. A*, Vol. 146, No. 3, pp. 311–318, 1983.
10. Izenman, A.J., “J.R. Wolf and the Zürich Sunspot Relative Numbers,” *Math. Intell.*, Vol. 7, No. 1, pp. 27–33, 1985.
11. Hoyt, D.V.; and Schatten, K.H.: *The Role of the Sun in Climate Change*, Oxford University Press, New York, NY, 288 pp., 1997.
12. Schröder, W.: “Some aspects of the earlier history of solar-terrestrial physics,” *Planet. Space Sci.*, Vol. 45, No. 3, pp. 395–400, doi:10.1016/S0032-0633(96)00119-5, March 1997.

13. Wilson, R.M.: "A Comparison of Wolf's Reconstructed Record of Annual Sunspot Number with Schwabe's Observed Record of 'Clusters of Spots' for the Interval 1826–1868," *Sol. Phys.*, Vol. 182, No. 1, pp. 217–230, doi:10.1023/A:1005046820210, January 1998.
14. Willson, R.C.; and Hudson, H.S.: "The Sun's luminosity over a complete solar cycle," *Nature*, Vol. 351, No. 6321, pp. 42–44, doi:10.1038/351042a0, May 2, 1991.
15. Wilson, R.M.: "On the Variation of the Nimbus-7 Total Solar Irradiance," NASA TP-3316, Marshall Space Flight Center, AL, 17 pp., December 1992.
16. Willson, R.C.: "Total solar irradiance trend during solar cycles 21 and 22," *Science*, Vol. 277, No. 5334, pp. 1963–1965, doi:10.1126/science.277.5334.1963, September 26, 1997.
17. Lean, J.; and Rind, D.: "Climate Forcing by Changing Solar Radiation," *J. Climate*, Vol. 11, No. 12, pp. 3069–3094, December 1998.
18. Fröhlich, C.; and Lean, J.: "The Sun's total irradiance: Cycles, trends, and related climate change uncertainties since 1976," *Geophys. Res. Lett.*, Vol. 25, No. 23, pp. 4377–4380, doi:10.1029/1998GL900157, December 1, 1998.
19. Willson, R.C.; and Mordvinov, A.V.: "Secular total solar irradiance trend during solar cycles 21–23," *Geophys. Res. Lett.*, Vol. 30, No. 5, pp. 21–23, doi:10.1029/2002GL016038, March 2003.
20. Pap, J.M.; Fox, P.; Fröhlich, C.; et al. (eds.): *Solar Variability and Its Effect on Climate*, *Geophys. Monogr. Ser.*, Vol. 141, American Geophysical Union, Washington, DC, 366 pp., 2004.
21. Mendoza, B.: "Total solar irradiance and climate," *Adv. Space Res.*, Vol. 35, No. 5, pp. 882–890, doi:10.1016/j.asr.2004.10.011, 2005.
22. Foukal, P.; Fröhlich, C.; Spruit, H.; and Wigley, T.M.L.: "Variations in solar luminosity and their effect on the Earth's climate," *Nature*, Vol. 443, pp. 161–166, doi:10.1038/nature05072, September 14, 2006.
23. Fröhlich, C.: "Total solar irradiance variations since 1978," *Adv. Space Res.*, Vol. 29, No. 10, pp. 1409–1416, doi:10.1016/s0273-1177(02)00203-x, 2002.
24. Fröhlich, C.: "Solar Irradiance Variability Since 1978: Revision of the PMOD Composite during Solar Cycle 21," *Space Sci. Rev.*, Vol. 125, Nos. 1–4, pp. 53–65, doi:10.1007/s11214-006-9046-5, August 2006.
25. Svensmark, H.; and Friis-Christensen, E.: "Variation of cosmic ray flux and global cloud coverage—a missing link in solar-climate relationships," *J. Atmos. Sol.-Terr. Phys.*, Vol. 59, No. 11, pp. 1225–1232, doi:10.1016/s1364-6826(97)00001-1, 1997.

26. Friis-Christensen, E.; and Svensmark, H.: “What do we really know about the Sun-climate connection?” *Adv. Space Res.*, Vol. 20, Nos. 4–5, pp. 913–921, 1997.
27. Beer, J.: “Long-term indirect indices of solar variability,” *Space Sci. Rev.*, Vol. 94, Nos. 1–2, pp. 53–66, doi:10.1023/A:1026778013901, November 2000.
28. Svensmark, H.: “Influence of Cosmic Rays on Earth’s Climate,” *Phys. Rev. Lett.*, Vol. 81, No. 22, pp. 5027–5030, doi:10.1103/PhysRevLett.81.5027, November 30, 1998.
29. Svensmark, H.: “Cosmic Rays and Earth’s Climate,” *Space Sci. Rev.*, Vol. 93, Nos. 1–2, pp. 175–185, doi:10.1023/A:1026592411634, July 2000.
30. Cliver, E.W.; Boriakoff, V.; and Feynman, J.: “Solar variability and climate change: Geomagnetic aa index and global surface temperature,” *Geophys. Res. Lett.*, Vol. 25, No. 7, pp. 1035–1038, doi:10.1029/98GL00499, April 1998.
31. Kishcha, P.V.; Dmitrieva, I.V.; and Obridko, V.N.: “Long-term variations of the solar-geomagnetic correlation, total solar irradiance, and northern hemispheric temperature (1868–1997),” *J. Atmos. Sol.-Terr. Phys.*, Vol. 61, No. 61, pp. 799–808, doi:10.1016/S1364-6826(99)00035-8, July 1999.
32. Bagó, E.P.; and Butler, C.J.: “The influence of cosmic rays on terrestrial clouds and global warming,” *Astron. Geophys.*, Vol. 41, No. 4, pp. 4.18–4.22, doi:10.1046/j.1468-4004.2000.00418.x, August 2000.
33. Wagner, G.; Livingstone, D.M.; Masarik, J.; et al.: “Some results relevant to the discussion of a possible link between cosmic rays and the Earth’s climate,” *J. Geophys. Res.*, Vol. 106, No. D4, pp. 3381–3387, doi:10.1029/2000JD900589, February 2001.
34. Carslaw, K.S.; Harrison, R.G.; and Kirkby, J.: “Cosmic Rays, Clouds, and Climate,” *Science*, Vol. 298, No. 5599, pp. 1732–1737, doi:10.1126/science.1076964, November 29, 2002.
35. Pallé, E.; and Butler, C.J.: “The proposed connection between clouds and cosmic rays: cloud behaviour during the past 50–120 years,” *J. Atmos. Sol.-Terr. Phys.*, Vol. 64, No. 3, pp. 327–337, doi:10.1016/S1364-6826(01)00105-5, February 2002.
36. Stozhkov, Y.I.: “The role of cosmic rays in the atmospheric processes,” *J. Phys. G: Nucl. Part. Phys.*, Vol. 29, No. 5, pp. 913–923, doi:10.1088/0954-3899/29/5/312, 2003.
37. Marsh, N.; and Svensmark, H.: “Solar Influence on Earth’s Climate,” *Space Sci. Rev.*, Vol. 107, Nos. 1–2, pp. 317–325, doi:10.1023/A:1025573117134, April 2003.
38. Kristjánsson, J.E.; Kristiansen, J.; and Kaas, E.: “Solar activity, cosmic rays, clouds, and climate—an update,” *Adv. Space Res.*, Vol. 34, pp. 407–415, doi:10.1016/j.asr.2003.02.040, 2004.

39. Harrison, R.G.: “Discrimination between cosmic ray and solar irradiance effects on clouds, and evidence for geophysical modulation of cloud thickness,” *Proc. R. Soc. A*, Vol. 464, No. 2098, pp. 2575–2590, doi:10.1098/rspa.2008.0081, October 2008.
40. Sloan, T.; and Wolfendale, A.W.: “Testing the proposed causal link between cosmic rays and cloud cover,” *Environ. Res. Lett.*, Vol. 3, No. 2, 6 pp., doi:10.1088/1748-9326/3/2/024001, 2008.
41. Erlykin, A.D.; Sloan, T.; and Wolfendale, A.W.: “Solar activity and the mean global temperature,” *Environ. Res. Lett.*, Vol. 4, No. 1, 5 pp., doi:10.1088/1748-9326/4/1/014006, 2009.
42. Dobrica, V.; Demetrescu, C.; and Maris, G.: “On the response of the European climate to solar/geomagnetic long-term activity,” *Ann. Geophys.-Italy*, Vol. 53, No. 4, pp. 39–48, doi:10.4401/ag-4552, 2010.
43. Mufti, S.; and Shah, G.N.: “Solar-geomagnetic activity influence on Earth’s climate,” *J. Atmos. Sol.-Terr. Phys.*, Vol. 73, No. 13, pp. 1607–1615, doi:10.1016/j.jastp.2010.12.012, August 2011.
44. Friis-Christensen, E.; and Lassen, K.: “Length of the Solar Cycle: An Indicator of Solar Activity Closely Associated with Climate,” *Science*, Vol. 254, No. 5032, pp. 698–700, doi:10.1126/science.254.5032.698, November 1991.
45. Butler, C.J.: “Maximum and minimum temperatures at Armagh Observatory, 1844–1992, and the length of the sunspot cycle,” *Sol. Phys.*, Vol. 152, pp. 35–42, doi:10.1007/978-94-011-0950-5\_6, 1994.
46. Keqian, Z.; and Butler, C.J.: “A Statistical Study of the Relationship between the Solar Cycle Length and Tree-Ring Index Values,” *J. Atmos. Sol.-Terr. Phys.*, Vol. 60, No. 18, pp. 1711–1718, doi:10.1016/S1364-6826(98)00142-4, December 1998.
47. Lassen, K.; and Friis-Christensen, E.: “Variability of the solar cycle length during the past five centuries and the apparent association with terrestrial climate,” *J. Atmos. Sol.-Terr. Phys.*, Vol. 57, No. 8, pp. 835–845, doi:10.1016/0021-9169(94)00088-6, July 1995.
48. Lassen, K.; and Friis-Christensen, E.: “Reply [to ‘Solar cycle lengths and climate: A reference revisited’],” *J. Geophys. Res.*, Vol. 105, No. A12, pp. 27,493–27,495, December 2000.
49. Laut, P.; and Gundermann, J.: “Solar cycle length hypothesis appears to support the ipcc on global warming,” *J. Atmos. Sol.-Terr. Phys.*, Vol. 60, No. 18, pp. 1719–1728, doi:10.1016/S1364-6826(98)00155-2, December 1998.
50. Fligge, M.; Solanki, S.K.; and Beer, J.: “Determination of solar cycle length variations using the continuous wavelet transform,” *Astron. Astrophys.*, Vol. 346, pp. 313–321, June 1999.

51. Reichel, R.; Thejll, P.; and Lassen, K.: “The cause-effect relationship of solar cycle length and the Northern Hemisphere air surface temperature,” *J. Geophys. Res.*, Vol. 106, No. A8, pp. 15,635–15,641, doi:10.1029/2001JA900027, August 2001.
52. Solanki, S.K.; Krivova, N.A.; Schüssler, M.; and Fligge, M.: “Search for a relationship between solar cycle amplitude and length,” *Astron. Astrophys.*, Vol. 396, pp. 1029–1035, doi:10.1051/0004-6361:20021436, 2002.
53. Kelly, P.M.; and Wigley, T.M.L.: “Solar cycle length, greenhouse forcing and global climate,” *Nature*, Vol. 360, pp. 328–330, doi:10.1038/360328a0, November 26, 1992.
54. Schlesinger, M.E.; and Ramankutty, N.: “Implications for global warming of intercycle solar irradiance variations,” *Nature*, Vol. 360, pp. 330–333, doi:10.1038/360330a0, November 26, 1992.
55. Soon, W.H.; Posmentier, E.S.; and Baliunas, S.L.: “Inference of solar irradiance variability from terrestrial temperature changes, 1880–1993: An astrophysical application of the Sun-climate connection,” *Astrophys. J.*, Vol. 472, pp. 891–902, doi:10.1086/178119, December 1996.
56. Laut, P.; and Gundermann, J.: “Solar cycle lengths and climate: A reference revisited,” *J. Geophys. Res.*, Vol. 105, No. A12, pp. 27,489–27,492, doi:10.1029/2000JA900068, December 2000.
57. Thejll, P.; and Lassen, K.: “Solar forcing of the Northern hemisphere land air temperature: New data,” *J. Atmos. Sol.-Terr. Phys.*, Vol. 62, No. 13, pp. 1207–1213, doi:10.1016/S1364-6826(00)00104-8, 2000.
58. Thejll, P.; and Lassen, K.: “Erratum to ‘Solar forcing of the Northern hemisphere land air temperature: new data,’” *J. Atmos. Sol.-Terr. Phys.*, Vol. 64, No. 1, p. 105, doi:10.1016/S1364-6826(01)00106-7, January 2002.
59. Laut, P.: “Solar activity and terrestrial climate: an analysis of some purported correlations,” *J. Atmos. Sol.-Terr. Phys.*, Vol. 65, No. 7, pp. 801–812, doi:10.1016/S1364-6826(03)00041-5, 2003.
60. Benestad, R.E.: “A review of the solar cycle length estimates,” *Geophys. Res. Lett.*, Vol. 32, No. 15, L15714, doi:10.1029/2005GL023621, August 2005.
61. Solheim, J.-E.; Stordahl, K.; and Humlum, O.: “The long sunspot cycle 23 predicts a significant temperature decrease in cycle 24,” *J. Atmos. Sol.-Terr. Phys.*, Vol. 80, pp. 267–284, doi:10.1016/j.jastp.2012.02.008, May 2012.
62. Loehle, C.: “Trend analysis of satellite global temperature data,” *Energy Environ.*, Vol. 20, No. 7, pp. 1087–1098, 2009.

63. de Jager, C.; and Duhau, S.: “Episodes of relative global warming,” *J. Atmos. Sol.-Terr. Phys.*, Vol. 71, pp. 194–198, doi:10.1016/j.jastp.2008.11.013, 2009.
64. Duhau, S.; and de Jager, C.: “The Forthcoming Grand Minimum of Solar Activity,” *J. Cosmol.*, Vol. 8, pp. 1983–1999, June 2010.
65. Feulner, G.; and Rahmstorf, S.: “On the effect of a new grand minimum of solar activity on the future climate on Earth,” *Geophys. Res. Lett.*, Vol. 37, No. 5, L05707, doi:10.1029/2010GL042710, March 2010.
66. Wilson, R.M.: “Solar Cycle and Anthropogenic Forcing of Surface-Air Temperature at Armagh Observatory, Northern Ireland,” NASA/TP—2010–216375, Marshall Space Flight Center, AL, 28 pp., March 2010.
67. Hoyt, D.V.; and Schatten, K.H.: “Group Sunspot Numbers: A New Solar Activity Reconstruction,” *Sol. Phys.*, Vol. 179, No. 1, pp. 189–219, doi:10.1023/A:1005007527816, April 1998.
68. Hoyt, D.V.; and Schatten, K.H.: “Group Sunspot Numbers: A New Solar Activity Reconstruction,” *Sol. Phys.*, Vol. 181, No. 2, pp. 491–512, doi:10.1023/A:1005056326158, August 1998.
69. Hathaway, D.H.; Wilson, R.M.; and Reichmann, E.J.: “Group Sunspot Numbers: Sunspot Cycle Characteristics,” *Sol. Phys.*, Vol. 211, Nos. 1–2, pp. 357–370, doi:10.1023/A:1022425402664, December 2002.
70. Kane, R.P.: “Some Implications Using the Group Sunspot Number Reconstruction,” *Sol. Phys.*, Vol. 205, No. 2, pp. 383–401, doi:10.1023/A:1014296529097, February 2002.
71. Faria, H.H.; Echer, E.; Rigozo, N.R.; et al.: “A comparison of the spectral characteristics of the Wolf sunspot number ( $R_z$ ) and group sunspot number ( $R_G$ ),” *Sol. Phys.*, Vol. 223, No. 1, pp. 305–318, doi:10.1007/s11207-004-5318-y, August 2004.
72. Hathaway, D.H.; and Wilson, R.M.: “What the Sunspot Record Tells Us About Space Climate,” *Sol. Phys.*, Vol. 224, Nos. 1–2, pp. 5–19, doi:10.1007/s11207-005-3996-8, October 2004.
73. Li, K.J.; Gao, P.X.; and Su, T.W.: “The Schwabe and Gleissberg Periods in the Wolf Sunspot Numbers and the Group Sunspot Numbers,” *Sol. Phys.*, Vol. 229, No. 1, pp. 181–198, doi:10.1007/s11207-005-5001-y, June 2005.
74. Butler, C.J.; and Johnston, D.J.: “The link between the solar dynamo and climate—the evidence from a long mean air temperature series from Northern Ireland,” *Irish Astron. J.*, Vol. 21, Nos. 3–4, pp. 251–254, 1994.
75. Butler, C.J.; and Johnston, D.J.: “A provisional long mean air temperature series for Armagh Observatory,” *J. Atmos. Sol.-Terr. Phys.*, Vol. 58, No. 15, pp. 1657–1672, doi:10.1016/0021-9169(95)00148-4, November 1996.



76. Coughlin, A.D.S.; and Butler, C.J.: “Is urban spread affecting the mean temperature at Armagh Observatory?” *Irish Astron. J.*, Vol. 25, No. 2, pp. 125–128, 1998.
77. Butler, C.J.; García Suárez, A.M.; Coughlin, A.D.S.; and Morrell, C.: “Air temperatures at Armagh Observatory, Northern Ireland, from 1796–2002,” *Int. J. Climatol.*, Vol. 25, pp. 1055–1079, doi:10.1002/joc.1148, 2005.
78. Wilson, R.M.; and Hathaway, D.H.: “Examination of the Armagh Observatory Annual Mean Temperature Record, 1844–2004,” NASA/TP—2006–214434, Marshall Space Flight Center, AL, 24 pp., July 2006.
79. Butler, C.J.; García Suárez, A.M.; Pallé, E.: “Trends and cycles in long Irish meteorological series,” *Biol. Environ.*, Vol. 107B, No. 3, pp. 157–165, December 2007.
80. Wilson, R.M.: “Evidence for solar-cycle forcing and secular variation in the Armagh Observatory temperature record (1844–1992),” *J. Geophys. Res.*, Vol. 103, No. D10, pp. 11,159–11,171, doi:10.1029/98JD00531, May 1998.
81. Hansen, J.R.; Sato, M.; Ruedy, R.; et al.: “Global temperature change,” *P. Natl. Acad. Sci. USA.*, Vol. 103, No. 39, pp. 14,288–14,293, doi:10.1073/pnas.0606291103, September 2006.
82. Hansen, J.R.; Ruedy, R.; Sato, M.; and Lo, K.: “Global surface temperature change,” *Rev. Geophys.*, Vol. 48, 29 pp., doi:10.1029/2010RG000345, December 2010.
83. Smith, E.M.: “Summary report on v1 vs v3 GHCN,” June 20, 2012, <<http://chiefio.wordpress.com/2012/06/20/summary-report-on-v1-vs-v3-ghcn/>>, accessed June 5, 2013.
84. Le Mouél, J.-L.; Blanter, E.; Shnirman, M.; and Courtillot, V.: “Evidence for solar forcing in variability of temperatures and pressures in Europe,” *J. Atmos. Sol.-Terr. Phys.*, Vol. 71, No. 12, pp. 1309–1321, doi:10.1016/j.jastp.2009.05.006, 2009.
85. Usoskin, I.G.; Solanki, S.K.; Schüssler, M.; et al.: “A Millennium-Scale Sunspot Number Reconstruction: Evidence for an Unusually Active Sun since the 1940s,” *Phys. Rev. Lett.*, Vol. 91, No. 21, 4 pp., doi:10.1103/PhysRevLett.91.211101, November 2003.
86. Solanki, S.K.; Usoskin, I.G.; Kromer, B.; et al.: “Unusual activity of the Sun during recent decades compared to the previous 11,000 years,” *Nature*, Vol. 431, pp. 1084–1087, doi:10.1038/nature02995, October 28, 2004.
87. Solanki, S.K.; Usoskin, I.G.; Kromer, B.; et al.: “Climate: How unusual is today’s solar activity? (reply),” *Nature*, Vol. 436, pp. E4–E5, doi:10.1038/nature04046, July 28, 2005.
88. Muscheler, R.; Joos, F.; Müller, S.A.; and Snowball, I.: “Climate: How unusual is today’s solar activity?” *Nature*, Vol. 436, pp. E3–E4, doi:10.1038/nature04045, July 28, 2005.

89. Lapin, L.L.: *Statistics for Modern Business Decisions*, 2nd ed., Harcourt Brace and Jovanovich, Inc., New York, NY, 788 pp., 1978.
90. Everitt, B.S.: *The Analysis of Contingency Tables*, John Wiley & Sons, New York, NY, 168 pp., 1977.
91. Wilson, R.M.; Hathaway, D.H.; and Reichmann, E.J.: "On Determining the Rise, Size, and Duration Classes of a Sunspot Cycle," NASA TP-3652, Marshall Space Flight Center, AL, 14 pp., September 1996.
92. Wilson, R.M.: "On the distribution of sunspot cycle periods," *J. Geophys. Res.*, Vol. 92, No. A9, pp. 10,101-10,104, doi:10.1029/JA092iA09p10101, September 1987.
93. Richards, M.T.; Rogers, M.L.; and Richards, D.S.P.: "Long-term Variability in the Length of the Solar Cycle," *Publ. Astron. Soc. Pacific*, Vol. 121, No. 881, pp. 797-809, doi:10.1086/604667, 2009.
94. Svalgaard, L.; Cliver, E.W.; and Kamide, Y.: "Sunspot cycle 24: Smallest cycle in 100 years?" *Geophys. Res. Lett.*, Vol. 32, L01104, doi:10.1029/2004GL021664, 2005.
95. de Jager, C.; and Dahau, S.: "Forecasting the parameters of sunspot cycle 24 and beyond," *J. Atmos. Sol.-Terr. Phys.*, Vol. 71, No. 2, pp. 239-245, doi:10.1016/j.jastp.2008.11.006, February 2009.
96. Wilson, R.M.; and Hathaway, D.H.: "Sunspot Activity Near Cycle Minimum and What It Might Suggest for Cycle 24, the Next Sunspot Cycle," NASA/TP-2009-216061, Marshall Space Flight Center, AL, 60 pp., September 2009.
97. Wilson, R.M.: "An Estimate of the Size and Shape of Sunspot Cycle 24 Based on Its Early Cycle Behavior Using the Hathaway-Wilson-Reichmann Shape-Fitting Function," NASA/TP-2011-216461, Marshall Space Flight Center, AL, 32 pp., March 2011.
98. Wilson, R.M.: "Bimodality and the Hale Cycle," *Sol. Phys.*, Vol. 117, No. 2, pp. 269-278, doi:10.1007/BF00147248, September 1988.
99. Lockwood, M.; and Fröhlich, C.: "Recent oppositely directed trends in solar climate forcings and the global mean surface air temperature," *Proc. R. Soc. A*, Vol. 463, No. 2086, pp. 2447-2460, October 2007.
100. Lockwood, M.; and Fröhlich, C.: "Recent oppositely directed trends in solar climate forcings and the global mean surface air temperature. II. Different reconstructions of the total solar irradiance variation and dependence on response time scale," *Proc. R. Soc. A*, Vol. 464, No. 2094, pp. 1367-1385, June 2008.

101. Lockwood, M.: “Recent changes in solar outputs and the global mean surface temperature. III. Analysis of contributions to global mean air surface temperature rise,” *Proc. R. Soc. A*, Vol. 464, No. 2094, pp. 1387–1404, doi:10.1098/rspa.2007.0348, June 2008.
102. Mursula, K.; and Ulich, Th.: “A new method to determine the solar cycle length,” *Geophys. Res. Lett.*, Vol. 25, No. 11, pp. 1837–1840, doi:10.1029/98GL51317, June 1998.
103. Wilson, R.M.; and Hathaway, D.H.: “Anticipating Cycle 24 Minimum and its Consequences: An Update,” NASA/TP—2008–215576, Marshall Space Flight Center, AL, 48 pp., October 2008.
104. Wilson, R.M.: “Variation of surface air temperatures in relation to El Niño and cataclysmic volcanic eruptions, 1796–1882,” *J. Atmos. Sol.-Terr. Phys.*, Vol. 61, pp. 1307–1319, doi:10.1016/S1364-6826(99)00055-3, February 1999.
105. Robock, A.: “Volcanic eruptions and climate,” *Rev. Geophys.*, Vol. 38, No. 2, pp. 191–219, doi:10.1029/1998RG000054, May 2000.
106. Santer, B.D.; Wigley, T.M.L.; Doutriaux, C.; et al.: “Accounting for the effects of volcanoes and ENSO in comparisons of modeled and observed temperature trends,” *J. Geophys. Res.*, Vol. 106, No. D22, pp. 28,033–28,059, doi:10.1029/2000JD000189, November 2001.
107. Collins, M.; An, S.-I.; Cai, W.; et al.: “The impact of global warming on the tropical Pacific Ocean and El Niño,” *Nat. Geosci.*, Vol. 3, pp. 391–397, doi:10.1038/NGEO868, June 2010.
108. Wilson, R.M.: “A Comparative Look at Sunspot Cycles,” NASA TP–2325, Marshall Space Flight Center, AL, 116 pp., May 1984.
109. Wilson, R.M.; Hathaway, D.H.; and Reichmann, E.J.: “On the behavior of the sunspot cycle near minimum,” *J. Geophys. Res.*, Vol. 101, No. A9, pp. 19,967–19,972, September 1996.
110. Rajamoorthy, M.; Duraisamy, P.; Pazhaniswami, J.R.; and Selvarajan, P.: “Influence of the solar activity on global temperature,” *World J. Sci. Technol.*, Vol. 1, No. 6, pp. 7 pp., 2011.
111. Schlesinger, M.E.; and Ramankutty, N.: “An oscillation in the global climate system of period 65–70 years,” *Nature*, Vol. 367, No. 6465, pp. 723–726, doi:10.1038/367723a0, February 1994.
112. Dijkstra, H.A.; te Raa, L.; Schmeits, M.; and Gerrits, J.: “On the physics of the Atlantic Multi-decadal Oscillation,” *Ocean Dynam.*, Vol. 56, No. 1, pp. 36–50, doi:10.1007/s10236-005-0043-0, May 2006.
113. Hofmann, D.J.; Butler, J.H.; Dlugokencky, E.J.; et al.: “The role of carbon dioxide in climate forcing from 1979 to 2004: introduction of the Annual Greenhouse Gas Index,” *Tellus B*, Vol. 58, No. 5, pp. 614–619, doi:10.1111/j.1600-0889.2006.00201.x, November 2006.

114. Lacis, A.A.; Schmidt, G.A.; Rind, D.; and Ruedy, R.A.: “Atmospheric CO<sub>2</sub>: Principal Control Knob Governing Earth’s Temperature,” *Science*, Vol. 330, No. 6002, pp. 356–359, doi:10.1126/science.1190653, October 2010.
115. Serreze, M.C.: “Understanding recent climate change,” *Conserv. Bio.*, Vol. 24, No. 1, pp. 10–17, doi:10.1111/j.1523-1739.2009.01408.x, February 2010.
116. Kaufmann, R.K.; Kauppi, H.; Mann, M.L.; and Stock, J.H.: “Reconciling anthropogenic climate change with observed temperature 1998–2008,” *P. Natl. Acad. Sci. USA.*, Vol. 108, No. 29, pp. 11,790–11,793, doi:10.1073/pnas.1102467108, July 2011.
117. Montzka, S.A.; Dlugokencky, E.J.; and Butler, J.H.: “Non-CO<sub>2</sub> greenhouse gases and climate change,” *Nature*, Vol. 476, No. 7358, pp. 43–50, doi:10.1038/nature10322, August 2011.
118. Keeling, C.D.; Bacastow, R.B.; Bainbridge, A.E.; et al.: “Atmospheric carbon dioxide variations at Mauna Loa Observatory, Hawaii,” *Tellus*, Vol. 28, No. 6, pp. 538–551, doi:10.1111/j.2153-3490.1976.tb00701.x, December 1976.
119. Bacastow, R.B.; Keeling, C.D.; and Whorf, T.P.: “Seasonal amplitude increase in atmospheric CO<sub>2</sub> concentration at Mauna Loa, Hawaii, 1959–1982,” *J. Geophys. Res.*, Vol. 90, pp. 10,529–10,540, doi:10.1029/JD090iD06p10529, October 1985.
120. Thoning, K.W.; Tans, P.P.; and Komhyr, W.D.: “Atmospheric carbon dioxide at Mauna Loa Observatory: 2. Analysis of the NOAA GMCC data, 1974–1985,” *J. Geophys. Res.*, Vol. 94, No. D6, pp. 8549–8565, doi:10.1029/JD094iD06p08549, June 1989.
121. Vitousek, P.M.: “Beyond Global Warming: Ecology and Global Change,” *Ecology*, Vol. 75, No. 7, pp. 1861–1876, doi:10.2307/1941591, October 1994.
122. Welch, D.W.; Ishida, Y.; and Nagasawa, K.: “Thermal limits and ocean migrations of sock-eye salmon (*Oncorhynchus nerka*): long-term consequences of global warming,” *Can. J. Fish. Aquat. Sci.*, Vol. 55, No. 4, pp. 937–948, doi:10.1139/f98-023, April 1998.
123. Rind, D.: “Complexity and Climate,” *Science*, Vol. 284, No. 5411, pp. 105–107, doi:10.1126/science.284.5411.105, April 1999.
124. Hughes, L.: “Biological consequences of global warming: is the signal already apparent?” *Trends Ecol. Evol.*, Vol. 15, No. 2, pp. 56–61, doi:10.1016/S0169-5347(99)01764-4, February 2000.
125. Karl, T.R.; and Trenberth, K.E.: “Modern Global Climate Change,” *Science*, Vol. 302, pp. 1719–1723, doi:10.1126/science.1090228, December 5, 2003.
126. Faris, S.: *Forecast: The Consequences of Climate Change, from the Amazon to the Arctic, from Darfur to Napa Valley*, Henry Holt and Company, New York, NY, 242 pp., 2009.

127. Karl, T.R.; Melillo, J.M.; and Peterson, T.C. (eds.): *Global Climate Change Impacts in the United States*, Cambridge University Press, New York, NY, 189 pp., 2009.
128. Rahmstorf, S.; and Coumou, D.: “Increase of extreme events in a warming world,” *Proc. Natl. Acad. Sci. USA.*, Vol. 108, No. 44, pp. 17,905–17,909, doi:10.1073/pnas.1101766108, October 2011.
129. Jones, P.D.: “Recent warming in global temperature series,” *Geophys. Res. Lett.*, Vol. 21, No. 12, pp. 1149–1152, doi:10.1029/94GL01042, June 1994.
130. Fasullo, J.T.; and Trenberth, K.E.: “A Less Cloudy Future: The Role of Subtropical Subsidence in Climate Sensitivity,” *Science*, Vol. 338, No. 6108, pp. 792–794, doi:10.1126/science.1227465, November 9, 2012.
131. Akasofu, S.-I.: “On the recovery from the Little Ice Age,” *Natural Science*, Vol. 2, No. 11, pp. 1211–1224, doi:10.4236/ns.2010.211149, November 2010.
132. Stauning, P.: “Solar activity–climate relations: A different approach,” *J. Atmos. Sol.-Terr. Phys.*, Vol. 73, No. 13, pp. 1999–2012, doi:10.1016/j.jastp.2011.06.011, August 2011.

REPORT DOCUMENTATION PAGE			Form Approved OMB No. 0704-0188		
<p>The public reporting burden for this collection of information is estimated to average 1 hour per response, including the time for reviewing instructions, searching existing data sources, gathering and maintaining the data needed, and completing and reviewing the collection of information. Send comments regarding this burden estimate or any other aspect of this collection of information, including suggestions for reducing this burden, to Department of Defense, Washington Headquarters Services, Directorate for Information Operation and Reports (0704-0188), 1215 Jefferson Davis Highway, Suite 1204, Arlington, VA 22202-4302. Respondents should be aware that notwithstanding any other provision of law, no person shall be subject to any penalty for failing to comply with a collection of information if it does not display a currently valid OMB control number.</p> <p><b>PLEASE DO NOT RETURN YOUR FORM TO THE ABOVE ADDRESS.</b></p>					
1. REPORT DATE (DD-MM-YYYY) 01-07-2013		2. REPORT TYPE Technical Publication		3. DATES COVERED (From - To)	
4. TITLE AND SUBTITLE Estimating the Mean Annual Surface Air Temperature at Armagh Observatory, Northern Ireland, and the Global Land-Ocean Temperature Index for Sunspot Cycle 24, the Current Ongoing Sunspot Cycle			5a. CONTRACT NUMBER		
			5b. GRANT NUMBER		
			5c. PROGRAM ELEMENT NUMBER		
6. AUTHOR(S)  Robert M. Wilson			5d. PROJECT NUMBER		
			5e. TASK NUMBER		
			5f. WORK UNIT NUMBER		
7. PERFORMING ORGANIZATION NAME(S) AND ADDRESS(ES) George C. Marshall Space Flight Center Huntsville, AL 35812			8. PERFORMING ORGANIZATION REPORT NUMBER  M-1360		
9. SPONSORING/MONITORING AGENCY NAME(S) AND ADDRESS(ES) National Aeronautics and Space Administration Washington, DC 20546-0001			10. SPONSORING/MONITOR'S ACRONYM(S) NASA		
			11. SPONSORING/MONITORING REPORT NUMBER NASA/TP-2013-217484		
12. DISTRIBUTION/AVAILABILITY STATEMENT Unclassified-Unlimited Subject Category 47 Availability: NASA CASI (443-757-5802)					
13. SUPPLEMENTARY NOTES  Prepared by the Science and Research Office, Science and Technology Office					
14. ABSTRACT  Estimates are given for the average annual mean surface air temperature at Armagh Observatory, Northern Ireland, and the Global Land-Ocean Temperature Index for sunspot cycle 24, the current ongoing sunspot cycle. The relationships between the temperatures and various markers of the sunspot cycle are also investigated to determine the relative strength of solar forcing now taking place. It is quite apparent that factors other than only solar forcing now dominate Earth's climate system (from sunspot cycle 21 onwards).					
15. SUBJECT TERMS Armagh surface air temperature, Global Land-Ocean Temperature Index, climate change, Atlantic Multi-decadal Oscillation, atmospheric concentration of carbon dioxide, sunspot cycle 24, temperature forecast					
16. SECURITY CLASSIFICATION OF:			17. LIMITATION OF ABSTRACT  UU	18. NUMBER OF PAGES  60	19a. NAME OF RESPONSIBLE PERSON STI Help Desk at email: help@sti.nasa.gov
a. REPORT  U	b. ABSTRACT  U	c. THIS PAGE  U			19b. TELEPHONE NUMBER (Include area code) STI Help Desk at: 443-757-5802



National Aeronautics and  
Space Administration  
IS20  
**George C. Marshall Space Flight Center**  
Huntsville, Alabama 35812

---